

Analysis of Character Correlations Among Wood Decay Mechanisms, Mating Systems, and Substrate Ranges in Homobasidiomycetes

DAVID S. HIBBETT¹ AND MICHAEL J. DONOGHUE

Harvard University Herbaria, Department of Organismic and Evolutionary Biology, Harvard University, 22 Divinity Avenue, Cambridge, Massachusetts 02138, USA

Abstract.—Homobasidiomycetes include the majority of wood-decaying fungi. Two basic forms of wood decay are known in homobasidiomycetes: white rot, in which lignin and cellulose are degraded, and brown rot, in which lignin is not appreciably degraded. An apparent correlation has been noted between production of a brown rot, decay of conifer substrates, and possession of a bipolar mating system (which has a single mating-type locus, in contrast to tetrapolar systems, which have two mating-type loci). The goals of this study were to infer the historical pattern of transformations in decay mode, mating type, and substrate range characters, and to determine if a causal relationship exists among them. Using nuclear and mitochondrial rDNA sequences, we performed a phylogenetic analysis of 130 species of homobasidiomycetes and performed ancestral state reconstructions by using parsimony on a range of trees, with various loss:gain cost ratios. We evaluated pairwise character correlations by using the concentrated changes test (CCT) of Maddison and the maximum likelihood (ML) method of Pagel. White rot, tetrapolar mating systems, and the ability to decay conifers and hardwoods appear to be plesiomorphic in homobasidiomycetes, whereas brown rot, bipolar mating systems, and exclusive decay of conifers appear to have evolved repeatedly. The only significant correlation among characters was that between brown rot (as the independent character) and exclusive decay of conifer substrates ($P < 0.03$). This correlation was supported by the CCT on a range of plausible trees, although not with every reconstruction of ancestral states, and by the ML test. Our findings suggest that the evolution of brown rot has promoted repeated shifts to specialization for conifer substrates. [Ancestral state reconstruction; basidiomycetes; comparative methods; concentrated changes test; Discrete; fungal ecology; Polyporaceae; rDNA; sensitivity analyses; wood decay.]

The vast majority of terrestrial biomass takes the form of wood and other plant tissues. The monumental task of recycling the carbon sequestered in wood falls primarily to homobasidiomycetes, which include ~13,000 described species of mushrooms and related macrofungi. Other fungi, such as ascomycetes and heterobasidiomycetes, and certain bacteria are also involved in wood decay but to a lesser extent. Two principal modes of wood decay are recognized in the homobasidiomycetes: white rot and brown rot (Rayner and Boddy, 1988; Worrall et al., 1997). White rot fungi degrade both lignin and cellulose (the major components of plant cell walls), leaving the substrate bleached and with a stringy consistency (Blanchette, 1991). In contrast, brown rot fungi selectively remove cellulose but do not appreciably degrade lignin. After colonization by brown rot fungi, the substrate has a reddish-brown color and a soft, crumbly consistency. Brown rot residues are highly resistant to further decomposition and make up a major

component of humic soils, especially in temperate and boreal forests (Gilbertson, 1980).

The origin and diversification of wood decay mechanisms in homobasidiomycetes has had a large impact on terrestrial ecosystems. In this study, we inferred phylogenetic relationships of homobasidiomycetes and the historical pattern of transformations between white rot and brown rot modes of wood decay. Using phylogenetic comparative methods, we evaluated previously proposed ecological and genetic correlates of decay modes. The general goal of this study was to understand some of the causal factors that have shaped the evolution of forested ecosystems.

Taxonomic Distribution and Correlates of Decay Modes

The mode of wood decay has been an important taxonomic character in homobasidiomycetes, especially in the predominantly wood-decaying polypores and corticioid fungi (crustlike, resupinate forms; Nobles, 1965, 1971; Stalpers, 1978; Gilbertson, 1980; Redhead and Ginns, 1985; Nakasone, 1990). Wood decay mode has generally been

¹Present address and address for correspondence: Biology Department, Clark University, Worcester, MA 01610 USA; E-mail: dhibbett@black.clarku.edu

regarded as a moderately conservative character and has often been used to differentiate genera. For example, Redhead and Ginns (1985) segregated the brown rot gilled mushroom genus *Neolentinus* from *Lentinus*, which is otherwise composed of white rot species. Similarly, Gilbertson and Ryvardeen (1986) distinguished the brown rot polypore genus *Antrodiella* from the morphologically similar white rot genus *Antrodiella*.

White rot is by far the more common form of wood decay in the homobasidiomycetes. Gilbertson (1980) estimated that 1,568 species of wood-decaying homobasidiomycetes have been described from North America, whereas only 103 species (7%) produce a brown rot (Table 1). According to Gilbertson (1980), 71 species (70%) of the North American brown rot fungi are in the Polyporaceae s. lat., which has long been regarded as an artificial taxon (Donk, 1964). According to the dominant morphology-based taxonomies of homobasidiomycetes (Donk, 1964; Singer, 1986), the remaining brown rot homobasidiomycetes are classified in six additional families: Coniophoraceae, Corticiaceae, Paxillaceae, Sparassidaceae, Stereaceae, and Tricholomataceae. Except for the Sparassidaceae, which has only two species in North America, each family that contains brown rot species also contains white rot species (Table 1). Recent molecular studies (reviewed by Hibbett and Thorn, 2001) suggest that five of the families that contain brown rot species (Corticiaceae, Paxillaceae, Polyporaceae, Stereaceae, and Tricholomataceae) are polyphyletic.

Because brown rot fungi are few in number and occur in taxonomically disparate groups, Gilbertson (1980) suggested that brown rot has been repeatedly derived from white rot.

TABLE 1. Distribution of brown rot fungi in families of homobasidiomycetes in North America, after Gilbertson^a (1980).

Family	No. brown rot species	No. white rot species
Coniophoraceae	14	6
Corticiaceae	5	291
Paxillaceae	4	8
Polyporaceae	71	297
Sparassidaceae	2	0
Stereaceae	3	17
Tricholomataceae	4	137

^aGilbertson also listed two species of Coprinaceae as producing a brown rot, but this has been refuted (Redhead and Ginns, 1985).

In contrast, Nobles (1965, 1971) suggested that brown rot is the plesiomorphic form in the homobasidiomycetes, and that white rot has been repeatedly derived by elaboration of wood decay mechanisms (i.e., gaining the ability to degrade lignin). Most recent authors have supported Gilbertson's view that the brown rot fungi are derived (Ryvardeen, 1991; Worrall et al., 1997; but see Watling, 1982); however, these inferences have not been based on phylogenetic analyses. Indeed, the lack of a broad phylogenetic classification of homobasidiomycetes has been the primary obstacle to understanding the evolution of decay modes (Rayner and Boddy, 1988). The artificial nature of the Polyporaceae is especially limiting, owing to the concentration of brown rot taxa in this family (Table 1).

Gilbertson (1980, 1981) and others have noted an apparent correlation between production of a brown rot and decay of conifer substrates. On the basis of monographs and floristic treatments by Overholts (1953) and Lowe (1966), Gilbertson (1980) estimated that 85% (60 species) of the brown rot-producing polypores in North America occur on conifer substrates. The relative frequencies of brown rot and white rot fungi on specific conifer and hardwood hosts also suggest that brown rot fungi are preferentially associated with conifers. Looking at seven species of conifers, Gilbertson (1980) found that, on average, 206 species of homobasidiomycetes decayed each host, of which 24% were brown rot fungi. In contrast, in seven species of hardwoods, an average of 114 species of homobasidiomycetes decayed each host, of which only 7% were brown rot fungi.

Another apparent correlation has been noted between the production of a brown rot and the presence of a bipolar mating system (an outcrossing mating system, in which mating compatibility is governed by a single locus, in contrast to tetrapolar systems, in which compatibility is governed by two loci). Determination of mating compatibility in homobasidiomycetes requires laboratory crossing studies with labor-intensive microscopic observations of hyphal septa. Nevertheless, mating type has been used as a taxonomic character, especially in wood-decaying fungi (e.g., Stalpers, 1978; Nakasone, 1990). The data Esser (1967) compiled on mating systems in 335 species of homobasidiomycetes suggested that ~25%

of homobasidiomycetes are bipolar, 65% are tetrapolar, and 10% are homothallic (selfing). Gilbertson (1980:34) noted that "all of the brown-rot fungi in the Polyporaceae tested to date are bipolar," and that "Only *Dacryobolus sudans* in the Corticiaceae and *Veluticeps berkeleyi* Cooke ex Pat. in the Stereaceae are known to be tetrapolar brown rotters." Ryvardeen (1991) confirmed the general pattern of association between brown rot and bipolar mating systems, although he also listed two brown rot tetrapolar homobasidiomycetes in the Polyporaceae (*Amylocystis lapponica* and *Parmastomyces transmutans*). As with wood decay modes, the evolutionary polarity of transformations between mating systems remains controversial. Some authors have suggested that bipolar mating systems are plesiomorphic (Nobles, 1971; Ryvardeen, 1991), but others conclude they have been repeatedly derived from tetrapolar systems (Raper and Flexer, 1971; Hibbett and Thorn, 2001).

Gilbertson (1980) proposed a hypothesis to explain the apparent correlation between brown rot, bipolarity, and decay of conifer substrates. Considering that conifer-dominated habitats, such as high-altitude or boreal forests, have shorter growing seasons than do hardwood-dominated habitats, he reasoned there would be selection for accelerated life cycles in conifer-dominated habitats. For reasons explained below, Gilbertson suggested that fungi with brown rot decay mechanisms and bipolar mating systems would have accelerated life cycles relative to fungi with white rot decay mechanisms or tetrapolar mating systems. In the present study, we used the concentrated changes test (CCT) of Maddison (1990; Maddison and Maddison, 1992) and the maximum likelihood (ML) method of Pagel (1994, 1997) to evaluate potential evolutionary correlations among these characters. Because these methods require pairwise comparisons of discrete characters, we have restated Gilbertson's hypothesis as a series of testable hypotheses involving pairs of characters:

Brown rot versus decay of conifer substrates.—Citing laboratory studies of wood decay, Gilbertson suggested that brown rot fungi decay wood more rapidly than white rot fungi. Therefore, he reasoned that brown rot fungi would have a fitness advantage over white rot fungi in conifer-dominated forests. An alternative explanation of why

brown rot fungi are preferentially associated with conifers could be that some physical or chemical property of conifer wood makes it more accessible to brown rot fungi than to white rot fungi. For example, Rayner and Boddy (1988:27–28) suggested that "the relatively more refractory nature of lignins of conifers may partly explain the more frequent occurrence of brown rot in wood of these trees than white rot." In either case, an association would be expected between evolution of brown rot and a shift onto conifer substrates. Gilbertson and Rayner and Boddy's hypotheses make no specific predictions about which character changed first. If evolution of brown rot promoted a shift onto conifer substrates, then we should expect to see a preponderance of shifts onto conifers nested within groups that have a brown rot. However, if the condition of growing on conifers promoted evolution of brown rot, then we should expect to find a preponderance of shifts to brown rot nested within clades that decay conifers.

Bipolar mating systems versus decay of conifer substrates.—Gilbertson predicted a correlation between bipolar mating systems and decay of conifer substrates for essentially the same reason that he predicted a correlation between brown rot and decay of conifers, namely, that bipolar mating systems result in an acceleration of the life cycle, which would confer a fitness advantage in conifer-dominated environments. The presumed reason for the acceleration is that the rate of formation of dikaryons, the effectively diploid, sexually reproducing stage of the homobasidiomycete life cycle, should be greater in bipolar than in tetrapolar species (because the haploid monokaryons of bipolar species can mate with half of their sibs, whereas those of tetrapolar species can mate with only one quarter of their sibs). Once again, Gilbertson's hypothesis makes no prediction about the order of evolution of the two characters; it simply predicts that evolution of bipolarity should be nonrandomly associated with shifts onto conifer substrates.

Brown rot versus bipolar mating systems.—Finally, Gilbertson's hypothesis predicts a correlation between the evolution of brown rot modes of wood decay and the evolution of bipolar mating systems. Gilbertson implied that the derivation of brown rot and bipolarity represent a general trend toward

genetic reduction (i.e., loss of genes). This idea was echoed by Worrall et al. (1997:217): "Thus, development of a brown-rot fungus from a white-rot fungus would be characterized, in large part, by simplification: conversion from a bifactorial [= tetrapolar] to unifactorial [= bipolar] mating system and loss of extracellular phenoloxidase and exoglucanase." However, Gilbertson's hypothesis does not imply any direct causal interaction between these characters; evolution of brown rot and evolution of bipolarity are supposedly correlated simply because they both contribute to an accelerated life cycle, which he suggested is favored in conifer-dominated forests.

MATERIALS AND METHODS

Taxa, Genes, and Molecular Techniques

We sampled 133 species of basidiomycetes (Table 2). The ingroup includes a diverse assemblage of 130 species of homobasidiomycetes representing 37 families of Hymenomycetes and Gasteromycetes in traditional, morphology-based classifications (Donk, 1964; Dring, 1973; Singer, 1986). Hibbett and Thorn (2001) proposed an informal phylogenetic classification, based on molecular phylogenies, that divides the homobasidiomycetes into eight major clades: polyporoid clade, euagarics clade, bolete clade, telephoroid clade, russuloid clade, hymenochaetoid clade, cantharelloid clade, and gomphoid-phalloid clade. All eight clades are represented in our data set (Table 3). However, from crude estimates of the number of described species in each clade (Hibbett and Thorn, 2001), a sampling bias is evident (Table 3). The most overrepresented group is the polyporoid clade, which includes 36% of the sampled taxa but represents only ~10% of described species of homobasidiomycetes. The most underrepresented group is the euagarics clade, which includes 17% of the sampled taxa but represents about 65% of described species of homobasidiomycetes, most of which are gilled mushrooms (Table 3; Hibbett and Thorn, 2001).

Three species of heterobasidiomycete "jelly fungi" were included for rooting purposes, including *Tremella foliacea* (Tremellales), *Dacrymyces chrysospermus* (Dacrymycetales), and *Auricularia auricula-judae* (Auriculariales). This choice of outgroups

is supported by analyses at more inclusive levels than the present study, which suggest that the heterobasidiomycetes make up a paraphyletic assemblage within which the homobasidiomycetes are nested (Swann and Taylor, 1993, 1995).

Sequence data were obtained from nuclear and mitochondrial small-subunit ribosomal RNA genes (nu-rDNA and mt-rDNA, respectively). Forty nu-rDNA and 31 mt-rDNA sequences were generated for the present study. The remaining sequences have been published previously (see Table 2 for references). Four species in the data set lack mt-rDNA sequences (*Laurilia sulcata*, *Neolentinus lepideus*, *Sparassis spathulata*, and *Tremella foliacea*) and seven species lack nu-rDNA sequences (*Acanthophysium cerrusatus*, *Gloeocystidiellum porosum*, *Phlebia tremellosa*, *Scytinostroma portentosum*, *Sistotrema sernanderi*, *Tulasnella pruinosa*, and *T. violea*). Most species have full-length nu-rDNA sequences, but 16 species have partial nu-rDNA sequences of ~0.6 kb, which align to a region between positions 567 and 1187 in the nu-rDNA of *Saccharomyces cerevisiae* (Table 2).

The primers and protocols used for polymerase chain reaction (PCR) amplification and sequencing have been described previously (White et al., 1990; Bruns and Szaro, 1992; Hibbett and Donoghue, 1995; Hibbett, 1996). Briefly, complete nu-rDNA genes (~1.8 kb) and partial mt-rDNA genes (0.5 kb to >1.0 kb) were amplified and sequenced directly by using dye-terminator cycle-sequencing chemistry (Applied Biosystems). Sequencing reactions were run on an ABI 377 automated DNA sequencer. Sequences were edited and contiguous sequences were assembled by using ABI Analysis software and Sequencher version 3.0 (GeneCodes Corp.). DNA sequences generated for this study have been deposited in GenBank (accession numbers AF334868-AF334940).

Alignment and Phylogenetic Analyses

DNA sequences were aligned by eye in the data editor of PAUP* 4.0 (Swofford, 1999). Hypervariable regions that were too divergent to be aligned were excluded from analyses (see Results and Discussion). A NEXUS file containing the aligned sequences has been deposited in TreeBASE (accession number 5580). For phylogenetic analyses, we used equally weighted parsimony

TABLE 2. Taxa, isolate codes, and sources of sequences.

Species, isolate number ^a	Sources of sequences ^b	
	mt-rDNA	nu-rDNA
<i>Abortiporus biennis</i> KEW 210	This study	This study
<i>Acanthophysium cerrusatus</i> FPL 11572	This study	No seq.
<i>Agaricus bisporus</i> DSH 96-057	C	G
<i>Albatrellus syringae</i> CBS 728.85	C	C
<i>Aleurodiscus botryosus</i> CBS 195.91	C	C
<i>Amanita muscaria</i> DUKE Moncalvo 96/63	C	C
<i>Amylostereum chailettii</i> FCUG 2025	This study	This study (0.6 kb)
<i>Amylostereum laevigatum</i> CBS 623.84	This study	This study
<i>Antrodia carbonica</i> DAOM 197828	A	B, C
<i>Antrodia xantha</i> KEW 43	This study	This study
<i>Auricularia auricula-judae</i> FPL 11504	A	H
<i>Auriporia aurea</i> FPL 7026	This study	This study
<i>Auriscalpium vulgare</i> DAOM 128994	A	B, this study
<i>Basidioradulum radula</i> TUB FO 23507a	C	C
<i>Bjerkandera adusta</i> DAOM 215869	A	B, this study
<i>Boletus satanas</i>	E	D
<i>Bondarzewia berkleyi</i> DSH 93-190	A	This study
<i>Bondarzewia montana</i> DAOM 415	A	B (1.2 kb)
<i>Botryobasidium isabellinum</i> GEL 2109	C	C
<i>Botryobasidium subcoronatum</i> GB 1286	C	C
<i>Calvatia gigantea</i> DSH 96-032	C	C
<i>Cantharellus tubaeformis</i> DSH 93-209	C	C
<i>Ceriporia purpurea</i> DAOM 213168	A	B, C
<i>Ceriporia viridans</i> FPL 7440	A	This study (0.6 kb)
<i>Ceriporiopsis subvermispora</i> FPL 90031	This study	This study
<i>Clavariadelphus pistillaris</i> TENN 37813	C	C
<i>Clavicornia pyxidata</i> THORN 752	B	B, C
<i>Clavulina cristata</i> DAOM 159321	C	C
<i>Coltricia perenis</i> DSH 93-198	A	B, C
<i>Coprinus</i> sp.	C	D
<i>Cortinarius iodes</i> DUKE Moncalvo 96/23	C	C
<i>Crucibulum laeve</i> DSH 96-02	C	C
<i>Cryptoporus volvatus</i> DAOM 211791	A	This study (0.6 kb)
<i>Cyathus striatus</i> DSH 96-001	C	C
<i>Dacrymyces chrysospermus</i> FPL 11353	C	H
<i>Daedalea quercina</i> DAOM 142475	A	B
<i>Daedaleopsis confragosa</i> DAOM 180496	A	This study (0.6 kb)
<i>Datronia mollis</i> DAOM 211792	A	This study (0.6 kb)
<i>Dendrocorticium roseocarenum</i> FPL 1800	This study	This study
<i>Dentipellis separans</i> CBS 538.90	This study	This study
<i>Dentocorticium sulphurellum</i> FPL 11801	C	C
<i>Dichostereum pallescens</i> CBS 717.81	This study	This study
<i>Echinodontium tinctorium</i> DAOM 16666	A	B, C
<i>Fistulina hepatica</i> DSH 93-183	A	B, C
<i>Fomes fomentarius</i> DAOM 129034	A	B, C
<i>Fomitopsis pinicola</i> DAOM 189134	A	B, C
<i>Ganoderma australe</i> DUKE Moncalvo 0705	C	C
<i>Gastrum saccatum</i> DSH 96-048	C	C
<i>Gloeocystidiellum leucoxantha</i> CBS 454.86	C	C
<i>Gloeocystidiellum porosum</i> CBS 510.85	This study	No seq.
<i>Gloeophyllum sepiarium</i> DAOM 137861	A	C
<i>Gloeoporus taxicola</i> KEW 213	This study	This study
<i>Gomphus floccosus</i> DSH 94-002	C	C
<i>Grifola frondosa</i> CBS 480.63	This study	This study
<i>Helicocybe sulcata</i> XXXXXX	This study	This study
<i>Henningsomyces candidus</i> THORN 156	This study	This study
<i>Hericium ramosum</i> DSH 93-199	A	B, C
<i>Heterobasidion annosum</i> DAOM 73191	A	B, C
<i>Hydnum</i> sp. DSH 96-008	C	C
<i>Hydnum repandum</i> EMP 96-001	C	C
<i>Hyphodontia alutaria</i> TUB GEL 2071	C	C
<i>Inonotus hispidus</i> FPL 3597	A	B, C

TABLE 2. Continued.

Species, isolate number ^a	Sources of sequences ^b	
	mt-rDNA	nu-rDNA
<i>Laetiporus portentosus</i> CIEFAP Rajchenberg 35	This study	This study
<i>Laetiporus sulphureus</i> DSH 93-194	A	B, C
<i>Laurilia sulcata</i> CBS 365.49	No seq.	This study
<i>Laxitextum bicolor</i> CBS 284.73	C	C
<i>Lentinellus omphalodes</i> DSH 9	A	B, C
<i>Lentinellus ursinus</i> VT 237	A	B, C
<i>Lentinula lateritia</i> DSH 92-143	A	B, C
<i>Lentinus tigrinus</i> DSH 93-181	A	B, C
<i>Lenzites betulina</i> DAOM 180504	A	This study (0.6 kb)
<i>Lepiota procera</i> DSH 96-038	C	G
<i>Lycoperdon</i> sp DSH 96-054	C	C
<i>Meripilus giganteus</i> DSH 93-193	A	C
<i>Multiclavula mucida</i> DSH 96-056	C	C
<i>Neolentinus lepidus</i> VT 306N	No seq.	This study
<i>Neolentiporus maculatissimus</i> CIEFAP Rajchenberg 158	This study	This study
<i>Oligoporus rennyi</i> KEW 57	This study	This study
<i>Ossicaulis lignatilis</i> DUKE 483	This study	This study
<i>Oxyporus</i> sp. DSH 93-188	A	C
<i>Panellus serotinus</i> DSH 93-218	A	C
<i>Panellus stypticus</i> DSH 93-213	A	C
<i>Panus rudis</i> DSH 92-139	C	C
<i>Paxillus panuoides</i> DSH 96-043	C	C
<i>Peniophora nuda</i> FPL 4756	A	C
<i>Perenniporia medulla panis</i> CBS 457.48	This study	This study
<i>Phaeolus schweinitzii</i> FPL 5096	A	C
<i>Phanerochaete chrysosporium</i> FPL 5175	A	C
<i>Phellinus gilvus</i> FPL 5528	A	This study (0.6 kb)
<i>Phellinus igniarius</i> FPL 5599	A	C
<i>Phlebia radiata</i> FPL 6140	C	C
<i>Phlebia tremellosa</i> FPL 4294	This study	No seq.
<i>Phylloporia ribis</i> FPL 10677	A	This study (0.6 kb)
<i>Piptoporus betulinus</i> DSH 93-186	A	This study (0.6 kb)
<i>Pleurotus</i> cf. <i>ostreatus</i> DSH 93-214	A	F
<i>Pleurotus tuberregium</i> DSH 92-155	A	This study
<i>Pluteus petasatus</i> DUKE Moncalvo 96/28	C	C
<i>Polyporus arcularius</i> DSH 92-144	A	This study (0.6 kb)
<i>Polyporus melanopus</i> DAOM 212269	A	This study (0.6 kb)
<i>Polyporus squamosus</i> FPL 6846	A	C
<i>Polyporus tuberaster</i> DAOM 7997B	A	This study (0.6 kb)
<i>Polyporus varius</i> DSH 93-195	A	This study (0.6 kb)
<i>Postia leucomallela</i> KEW 29	This study	This study
<i>Pseudocolus fusiformis</i> DSH 96-033	C	C
<i>Pulcherricium caeruleum</i> FPL 7658	A	This study
<i>Pycnoporus cinnabarinus</i> DAOM 72065	A	This study (0.6 kb)
<i>Ramaria stricta</i> TENN HDT-5474	C	C
<i>Russula compacta</i> DUKE s.n.	A	C
<i>Schizophyllum commune</i> DSH 96-026	C	D
<i>Schizopora paradoxa</i> TUB GEL 2511	C	C
<i>Scleroderma citrina</i> DSH 96-011	C	C
<i>Scytinostroma alutum</i> CBS 762.81	C	C
<i>Scytinostroma portentosum</i> CBS 503.48	This study	No seq.
<i>Sistotrema eximum</i> THORN 420	This study	This study
<i>Sistotrema musicola</i> FPL 8233	This study	This study
<i>Sistotrema sernanderi</i> CBS 926.70	This study	No seq.
<i>Sparassis spathulata</i> DSH 93-184	No seq.	C
<i>Sphaerobolus stellatus</i> DSH 96-015	C	C
<i>Stereum annosum</i> FPL 8562	A	C
<i>Stereum hirsutum</i> FPL 8805	A	C
<i>Stropharia rugosoannulata</i> DUKE 258	C	C
<i>Thelephora</i> sp. DSH 96-010	C	C
<i>Trametes suaveolens</i> DAOM 196328	A	C
<i>Trametes versicolor</i> DSH 93-197	A	This study (0.6 kb)

TABLE 2. Continued.

Species, isolate number ^a	Sources of sequences ^b	
	mt-rDNA	nu-rDNA
<i>Tremella foliacea</i>	No seq.	H
<i>Trichaptum abietinum</i> FPL 8973	A	C
<i>Tulasnella pruinosa</i> DAOM 17641	This study	No seq.
<i>Tulasnella violae</i> DAOM 222001	This study	No seq.
<i>Tulostoma macrocephala</i> FH Long 10111	C	C
<i>Typhula phacorhiza</i> DSH 96-059	C	C
<i>Tyromyces chioneus</i> KEW 141	This study	This study
<i>Vararia insolita</i> CBS 667.81	This study	This study
<i>Wolfiporia cocos</i> FPL 4198	This study	This study

^aApplies only to sequences generated in our laboratory. Prefixes indicate origin of isolates: CBS = Centraalbureau voor Schimmeltcultures, Baarn, The Netherlands; DAOM = Canadian Collection of Fungal Cultures, Ottawa, Canada; DSH = personal herbarium of David S. Hibbett; DUKE = Duke University Mycology culture collection and herbarium, Durham, NC; EMP = personal herbarium of Elizabeth M. Pine; FCUG = Department of Systematic Botany, University of Gothenberg, Sweden; FH = Farlow Herbarium, Cambridge; FPL = USDA Forest Products Laboratory, Madison, WI; KEW = Royal Botanic Gardens, Kew, U.K.; CIEFAP = collection of Mario Rajchenberg, Centro Forestal, Chubut, Argentina; TENN = Department of Botany, University of Tennessee, Knoxville; THORN = personal herbarium of R.G. Thorn; TUB = Department of Botany and Mycology, Tübingen University, Tübingen, Germany; VT = Department of Botany, Virginia Polytechnic Institute, Blacksburg.

^bA, Hibbett and Donoghue (1995); B, Hibbett (1996); C, Hibbett et al. (1997); D, Bruns et al. (1992); E, Bruns and Szaro (1992); F, Gargas et al. (1995); G, Hinkle et al. (1994); H, Swann and Taylor (1995). Full-length sequences, unless indicated otherwise.

in test versions of PAUP* 4.0 (4.0b1–4.0b2a; Swofford, 1999) run on Macintosh computers. Phylogenetic trees were inferred by using a two-step search protocol based on strategies described by Olmstead et al. (1993) and Maddison et al. (1992). In the first step of the analyses, 100 or more heuristic searches were performed, with random taxon addition sequences, MAXTREES set to autoincrease, TBR branch swapping, and retention of no more than two shortest trees per replicate. In the second step of the analyses, the shortest trees from the first step were used as starting trees for TBR branch swapping with MAXTREES set to 3,000. This general search protocol was followed in all parsimony analyses

(except those in the incongruence length difference [ILD] test, see below), varying only the number of replicate heuristic searches in the first step of the analysis. Topological robustness was estimated by bootstrap analysis (Felsenstein, 1985; Sanderson, 1995). Bootstrap analyses used 100 replicate heuristic searches, each with one random taxon addition sequence, TBR branch swapping, and retention of one tree per replicate.

Before combining the nu-rDNA and mt-rDNA data, we performed a series of analyses to assess the combinability of the data, using a 123-taxon core dataset that excluded all taxa that lacked either nu-rDNA or mt-rDNA data. Global and local tests of combinability

TABLE 3. Relative proportions of sampled species compared with described species.

Category	No. of species sampled in this study	Estimated actual proportions ^a
Polyporoid clade	47 (36.2%)	1,350 (10%)
Euagarics clade	22 (16.9%)	8,425 (65%)
Bolete clade	3 (2.3%)	840 (7%)
Theleporoid clade	2 (1.5%)	240 (2%)
Russuloid clade	26 (20.0%)	1,000 (8%)
Hymenochaetoid clade	10 (7.7%)	630 (5%)
Cantharelloid clade	10 (7.7%)	170 (1%)
Gomphoid-phalloid clade	6 (4.6%)	350 (3%)
Incertae sedis	4 (3.1%)	—
Saprotrophic/pathogenic species	115 (88.5%)	8,500 (65%)
Brown rot species	21 (18.3%) ^b	106 (7%) ^c

^aEstimates of total diversity of described species of homobasidiomycetes from Hibbett and Thorn (2001), based on species counts in Hawksworth et al. (1995), except where noted.

^bProportion of brown rot fungi calculated as percentage of saprotrophic/pathogenic species in the dataset.

^cProportion of brown rot fungi calculated as percentage of wood decaying homobasidiomycetes in North America (from Gilbertson, 1980).

were performed. To assess the global test of combinability we used the ILD test of Farris et al. (1994, 1995), implemented as the partition homogeneity test in PAUP*, with 100 replicates and all nucleotide positions included.

Local tests of incongruence were conducted to evaluate positive conflict involving individual nodes in trees derived from the independent data partitions. The first step in this process was to perform independent analyses of the mt-rDNA and nu-rDNA data partitions in the core dataset. The basic two-step search protocol outlined above was used, with 100 replicate searches in step one of the analysis. Bootstrap analyses were performed as described above. We evaluated conflicting nodes in the mt-rDNA and nu-rDNA trees, that is, nodes that were supported by 70% or more of the bootstrap replicates from one data partition but were positively incongruent with the strict consensus tree derived from the other data partition (regardless of its bootstrap support). For each potentially conflicting node, a constraint tree was constructed in MacClade version 3.0 (Maddison and Maddison, 1992) that forced monophyly of that node but specified no other topological structure. Constrained phylogenetic analyses were performed using only the first step of the general search protocol (i.e., 100 replicate searches with TBR, keeping only two trees per replicate), and the results were compared with unconstrained trees by using the Wilcoxon signed ranks test (WSR; Templeton, 1983) implemented in PAUP*.

After testing for incongruence, the data partitions were combined and subjected to parsimony analyses. Combined analyses of the core data set (with no missing data) used 100 replicate searches in step one of the analysis, whereas combined analyses of the full data set (including those taxa missing either nu-rDNA or mt-rDNA data) used 5,000 replicate searches in step one of the analysis. In the analysis of the full data set, individual islands of trees (Maddison, 1991) were delimited by swapping on the trees obtained in the first step of the analysis one at a time and using the "get trees" options to filter the remaining trees. Strict consensus trees were generated from all equally most-parsimonious trees, as well as from each set of trees representing one tree island (in analysis of the full data set only). Bootstrap analyses were performed

as described above. Transition/transversion ratios for the nu-rDNA and mt-rDNA data partitions were inferred with parsimony by using MacClade.

Constrained analyses of the full data set were performed to evaluate two alternative phylogenetic hypotheses that are suggested by morphology, as well as by decay mode and mating system characters. Constrained analyses used 1,000 replicate searches in step one of the analysis. Results of constrained and unconstrained analyses were compared by the WSR test. In each constrained analysis, only one node was constrained at a time. Constraint one forced *Gloeophyllum sepiarium*, *Heliocybe sulcata*, and *Neolentinus lepideus* to form a monophyletic group (hereafter referred to as the "Gloeophyllum clade") and a group of 14 other species, mostly polypores, that we call the "Antrodia clade" (see Results and Discussion). *Gloeophyllum*, *Neolentinus*, and *Heliocybe* share several characters with (most) members of the *Antrodia* clade, including production of a brown rot and bipolar mating system.

Constraint two forced monophyly of the members of the polyporeoid clade, *Gloeophyllum* clade, euagarics clade, bolete clade, theleporoid clade, and russuloid clade. This constraint reflects a hypothesis of higher-level phylogenetic relationships of homobasidiomycetes, based on an analysis of four rDNA regions (nuclear and mitochondrial large and small subunit rDNA) in a subset of the taxa used in this study (Hibbett, unpublished). This constraint is also congruent with comparative data on the ultrastructure of septal pores. As far as we know, all members that have been investigated of the groups united by this constraint have perforated parenthesomes (membrane-bound organelles that flank septal pores). In contrast, all members of the hymenochaetoid, cantharelloid, and gomphoid-phalloid clades that have been investigated, as well as many heterobasidiomycetes, have nonperforated parenthesomes—which appears to be the plesiomorphic condition of the homobasidiomycetes (Hibbett and Thorn, 2001).

Character Coding and Ancestral State Reconstruction

Ancestral states in decay mode, mating system, and substrate range characters were estimated with parsimony by

using MacClade (Maddison and Maddison, 1992). Characters were scored from literature sources (listed in the Appendix). In a few cases, we had to score species on the basis of reports regarding putatively closely related species. Thus, the mating type of *Stropharia rugosoannulata* was based on reports about *S. merdaria*, *S. semiglobata*, and *S. umbonatescens*; the mating type of *Dacrymyces chrysospermus* was based on *Cerinomyces spp.*; the mating type of *Dentocorticium sulphurellum* was based on *D. ussuricum*; and all characters of *Vararia insolita* were based on *V. sphericospora* and other *Vararia* species.

All characters were scored in binary form. "Decay mode" (0 = white rot, 1 = brown rot) was scored as missing (= uncertain) for 23 species, including 12 of 15 ectomycorrhizal species in the data set. However, the ectomycorrhizal species *Amanita muscaria*, which has been shown to degrade lignin (Trojanowski et al., 1984), was scored as having white rot. "Mating type" (0 = tetrapolar, 1 = bipolar) was scored as missing in 73 species, including four species that have been reported to be homothallic or simply heterothallic.

Two alternative characters were scored to represent substrate range. The first character, "conifer decay ability," was based on whether a species has ever been reported growing on conifer wood substrates (0 = not reported on conifer wood; 1 = reported on conifer wood). Ectomycorrhizal species were scored as 0. Two species for which data are insufficient were scored as missing: *Scytinostroma aluta* and *Multiclavula mucida*. The alternative character, "conifer exclusivity," was based on whether a species occurs exclusively as a saprotroph on conifer wood (0 = not exclusively on conifers, 1 = exclusively on conifers). No taxa were scored as missing. The two codings of substrate range differed in their treatment of taxa that occur on both conifers and hardwoods. Such taxa are coded 1 under conifer decay ability, whereas under conifer exclusivity they are coded 0.

Ancestral state reconstructions were performed for each character on trees derived from the unconstrained analysis of the full data set, as well as those derived from both of the constrained analyses. Each optimization was performed for a range of five loss:gain cost ratios (3:1, 2:1, 1:1, 1:2, 1:3), which were implemented by using step matrices. The goal of these exercises was to explore the sensitivity of ancestral state reconstructions to

alternative tree topologies (Donoghue and Ackerly, 1996) and assumptions regarding the cost of gains versus losses (Ree and Donoghue, 1999).

Correlation Analyses

We investigated potential correlations among three sets of organismal attributes: decay mode, mating system, and substrate range. Because there were two alternative codings of substrate range (conifer decay ability vs. conifer exclusivity), five pairwise interactions among characters had to be considered. In each case, there was no a priori hypothesis about which character in the pair should be considered dependent and which independent. Thus, 10 classes of comparative analyses could have been performed. To identify the pairs of characters that were most likely to be correlated, we inspected ancestral state reconstructions on tree 1 from the first island of trees discovered in the unconstrained analysis of the full data set, assuming equally weighted losses and gains. When the pattern of changes exhibited by a pair of characters suggested a causal relationship might exist between them, we tested the correlation by using the CCT, based on the most-parsimonious resolutions (MPRs) obtained with equally weighted losses and gains (Donoghue, 1989; Maddison, 1990; Maddison and Maddison, 1992; see below for details). Correlations found to be significant with the CCT were also evaluated by using the ML test in Discrete (Pagel, 1994; see below).

The CCT was performed with 1,000 simulations, MINSTATE character state reconstruction, and "compensation" set to 1. Significance was assessed by determining the probability of observing as many as, or more than, the inferred number of gains (and any number of losses) in the dependent character nested within the "distinguished" clades (Maddison and Maddison, 1992). Initial *P* values were multiplied by the number of tests to correct for multiple tests.

Often, we found more than one MPR for at least one of the characters in a pair. In addition, some reconstructions suggested changes in both the dependent and independent character along the same branch. In such cases, we performed the CCT by using two different MPRs, choosing those that maximized gains or losses, and used different

assumptions regarding the sequence of evolution in characters that were inferred to change on the same branch. The goal of these exercises was to test potential correlations among characters by using those patterns of character evolution that were most likely or least likely to support a correlation (Maddison and Maddison, 1992). We also examined the sensitivity of our results to alternative tree topologies; when significant results were obtained for tree 1 from island 1, we repeated the test, using one tree from each of the six other independent islands of most-parsimonious trees from the unconstrained analysis, as well as one tree from each of the two constrained analyses.

We used the ML method of Pagel (1994, 1997), implemented in Discrete (running under Windows NT), to evaluate the hypothesis that possession of brown rot promotes shifts onto conifer substrates (which was suggested by the CCT; see Results and Discussion). Discrete requires that all terminal taxa be scored for the characters of interest. Therefore, we coded the 23 species with missing values for wood decay according to the states inferred by using equally weighted parsimony optimization. The test was performed with tree 1 from the unconstrained analysis and with branch lengths set equal to the numbers of nucleotide substitutions inferred by parsimony. However, because Discrete does not tolerate zero-length branches, two zero-length terminal branches (leading to *Wolfiporia cocos* and *Laurilia sulcata*) were set to one step. Finally, the branch connecting the outgroup *Dacrymyces* to the rest of the taxa was arbitrarily rooted at its midpoint.

Discrete infers a model of evolution for two characters. The model parameters that Discrete estimates are the instantaneous transformation probabilities for each character, given a particular state in the other character; two characters would have eight separate parameters (Pagel, 1994). We estimated two models of evolution. In the first model, the probability of a gain in conifer exclusivity is independent of the state of wood decay. Accordingly, the parameter that defines the probability of a gain of conifer exclusivity when decay mode = white rot was restricted to being equal to the parameter that defines the probability of a gain of conifer exclusivity when decay mode = brown rot. Thus, there are seven free parameters in the first model. In the second model, the param-

eters are not restricted to being equal, which allows the probability of transformations to conifer exclusivity to vary according to the state of wood decay. The second model has eight free parameters. A branch-scaling parameter was also estimated for both classes of models. Thus, the two models are nested and have eight and nine free parameters, respectively (Pagel, 1994). The analysis for each model was repeated 10 times (with up to 25 iterations of the maximization steps in each analysis), and the optimal likelihood scores, $L(D_8)$ and $L(D_9)$, for each model were compared. The likelihood ratio statistic is twice the difference in $-\log L$ and is χ^2 distributed with one degree of freedom (Pagel, 1994).

RESULTS AND DISCUSSION

Sequence and Alignment Characteristics

In most isolates, PCR products of nu-rDNA were ~1.8 kb. However, as described previously (Hibbett, 1996), five species (*Lentinellus omphalodes*, *L. ursinus*, *Clavicornia pyxidata*, *Panellus stypticus*, and *Laetiporus portentosus*) have group 1 introns of ~400 bp, which are inserted at the same position in all species and were excised before alignment. In most taxa, the nu-rDNA sequences could be aligned with little ambiguity across their entire length. However, the nu-rDNA of *Cantharellus tubaeformis* contained three hypervariable regions of 54, 114, and 91 bp that could not be aligned to the other taxa in the study. After excluding the hypervariable regions of *Cantharellus* and trimming ~45 bp from the start and end of the alignment, the usable nu-rDNA sequences were 1,820 bp, including 737 (40%) variable positions and 434 (24%) parsimony-informative positions. The transition/transversion ratio in the nu-rDNA data partition (inferred with parsimony, based on tree 1 produced in the combined analysis of the full data set) was 1.895.

PCR products of mt-rDNA ranged from ~500 bp to >1 kb. This length variation reflects insertions and deletions in three hypervariable regions that are interspersed among four relatively conserved regions. This pattern of variable and conserved regions in mitochondrial small subunit rDNA has been described previously in fungi and other organisms (Gray et al., 1984; Bruns and Szaro, 1992; Hibbett and Donoghue, 1995). Sequences from the hypervariable regions were too divergent to be aligned except among

the most closely related taxa. Sequences of the conserved regions were aligned separately in four blocks, as described previously (Hibbett and Donoghue, 1995). The total aligned length of the conserved regions of mt-rDNA was 509 bp. Within the conserved regions, three regions of 6, 11, and 40 bp were deemed ambiguously aligned and were excluded from the analysis. After we excluded these regions and trimmed ~40 bp from the start of the alignment, the usable mt-rDNA sequences were 418 bp, including 339 (81%) variable positions, of which 267 (64%) were parsimony-informative. The inferred transition/transversion ratio in the mt-rDNA data partition was 0.881.

Independent Analyses and Tests of Combinability

Independent analyses of nu-rDNA or mt-rDNA each recovered large numbers of trees. The first step of the independent analysis of the nu-rDNA partition found two trees of 3,048 steps, which were hit once in 100 replicates. TBR swapping on these trees with MAXTREES set to 3,000 produced 3,000 trees of 3,047 steps (consistency index [CI] = 0.343, retention index [RI] = 0.534). The first step of the analysis of the mt-rDNA partition found four trees of 2,890 steps in two replicates. TBR swapping on these trees with MAXTREES set to 3,000 produced 3,000 trees of 2,888 steps (CI = 0.229, RI = 0.548). Results of the ILD test suggested that the nuclear and mitochondrial data partitions are significantly heterogeneous. The sum of the tree lengths from analyses of the original partitions (6,032 steps) was 69 steps shorter than the smallest sum of tree lengths from random partitions (6,101–6,198 steps; $P = 0.01$).

Because the ILD test suggested that the data partitions were heterogeneous, we performed constrained analyses with the WSR test in an effort to identify incongruent placements of taxa or clades, which might reflect different phylogenetic histories among the nuclear and mitochondrial rDNAs (de Queiroz et al., 1995). Eight nodes in the nu-rDNA tree that were supported by 70% or more of the bootstrap replicates positively conflict with the strict consensus of the mt-rDNA trees. Eight constrained analyses of the mt-rDNA partition were performed, each forcing the mt-rDNA tree to resolve one of the strongly supported conflicting nodes re-

solved by the analysis of nu-rDNA partition. Constrained analyses produced from one to eight trees each, ranging from 2,890 to 2,896 steps (2 to 8 steps longer than the unconstrained trees). None of the constrained trees was rejected by the WSR test ($P = 0.467$ – 0.925). Results of using the reciprocal analyses for the nu-rDNA data partition were similar. Eight nodes in the mt-rDNA tree that were supported by 70% or more of the bootstrap replicates positively conflict with the strict consensus of the nu-rDNA tree. Constrained analyses of the nu-rDNA data partition generated two to four trees each, which ranged from 3,049 to 3,055 steps (2 to 8 steps longer than the unconstrained trees), none of which was rejected by the WSR test ($P = 0.382$ – 0.981). Thus, even though the ILD test suggested that the mitochondrial and nuclear data partitions are significantly heterogeneous, using the WSR test we were unable to detect individual strongly conflicting nodes, which might reflect hybridization, lineage sorting, or horizontal transmission, and therefore we could not identify taxa or sequences that could have been pruned from the dataset to eliminate conflict (de Queiroz et al., 1995).

The significant result of the ILD test does not necessarily indicate that the nu-rDNA and mt-rDNA data partitions have different underlying phylogenies. Studies by Sullivan (1996) and Cunningham (1997) with empirical data from “known” phylogenies suggest that strong process heterogeneity (different rates of evolution) among datasets with identical histories (e.g., first and second vs. third codon positions, or linked mitochondrial genes) can cause the ILD test to indicate that the data sets are significantly heterogeneous. In the present study, the greater frequency of variable positions in mt-rDNA (81%) than nu-rDNA (40%), and the much lower inferred transition/transversion ratio in mt-rDNA (0.881) than in nu-rDNA (1.895), suggest that the mt-rDNA evolves faster than the nu-rDNA. Because we could not detect strong incongruence among individual nodes in the nu-rDNA and mt-rDNA trees with the WSR test, we infer that the results of the ILD test reflect evolutionary rate heterogeneity between the nu-rDNA and mt-rDNA.

On the basis of simulation studies, Bull et al. (1993) suggested that combining data sets with strong process heterogeneity can

reduce phylogenetic accuracy. However, using empirical data sets, Sullivan (1996) and Cunningham (1997) found that phylogenetic accuracy may be improved in combined analyses of data sets with strong process heterogeneity, even when the ILD test suggests that the data sets should not be combined. Sullivan (1996) suggested that the simulated sequence data in the study of Bull et al. (1993) may not realistically reflect the distribution of rate variation within and between real genes. Given the findings of Sullivan (1996) and Cunningham (1997), we do not think our ILD test results warrant keeping the mt-rDNA and nu-rDNA data separate.

Combined Analyses

Combined analyses of the core dataset.—Step one of the combined analysis of the core data set found two trees of 6,161 steps. TBR swapping on these trees produced 220 trees of 6,154 steps (CI = 0.277, RI = 0.517). The combined analysis recovered fewer equally most-parsimonious trees than either independent analysis and provided more phylogenetic resolution. One hundred seven nodes were resolved in the strict consensus of the combined analysis, whereas 85 nodes were resolved in the strict consensus of the independent analysis of the nu-rDNA partition and 91 nodes were resolved in strict consensus of the independent analysis of the mt-rDNA partition. In addition, the combined analysis recovered more strongly supported nodes, as measured by bootstrapping, than either independent analysis. In the combined analysis, the 50% majority rule bootstrap consensus tree had 54 nodes resolved, with 34 nodes supported by at least 75%. In contrast, in the nu-rDNA-only analysis, the 50% majority rule consensus tree had 31 nodes resolved, with 19 receiving 75% or better bootstrap support; in the mt-rDNA-only analysis, the 50% majority rule consensus tree had 36 nodes resolved, with 18 nodes receiving 75% or better support. These results suggest that the combined data set has a stronger phylogenetic signal than either independent data set. Similar results were obtained by Soltis et al. (1998), who found that combined analyses of linked chloroplast genes produced trees with greater resolution and support (and had faster run times) than independent analyses, even though the ILD

test suggested that the genes represented heterogeneous data partitions.

Combined analyses of the full data set.—Step one of the combined analysis of the full data set found 18 trees of 6,421 steps. TBR branch swapping on these trees produced 1,720 trees of 6,421 steps (CI = 0.273, RI = 0.526), which occur in seven TBR islands. The two largest islands (with 440 and 880 trees) were hit twice in the first step of the analysis, but the other islands (with 40 to 160 trees each) were hit only once.

The strict consensus of all equally most-parsimonious trees has a 17-way polytomy near the base of the homobasidiomycetes (Fig. 1). Inspection of the strict consensus trees from each of the tree islands showed that the reason for this polytomy is that *Dendrocorticium roseocarneum*, *Gloeocystidiellum porosum*, and the *Gloeophyllum* clade occur in widely separated parts of the tree in different islands (described below; Fig. 2). These taxa were pruned from the trees and the strict consensus was recalculated in PAUP* (no redundant trees were created by pruning; the pruned consensus tree is not shown). In the consensus of the pruned trees, the eight major clades of homobasidiomycetes described by Hibbett and Thorn (2001) were resolved. These eight clades are also resolved in the majority rule bootstrap tree from analyses that include all taxa, with the following levels of support: polyporoid clade = 27%, euagarics clade = 93%, bolete clade = 89%, theleporoid clade = 99%, russuloid clade = 49%, hymenochaetoid clade = 80%, cantharelloid clade = 74%, and gomphoid-phalloid clade = 100% (Fig. 1).

In islands 1–4 and 6 (totaling 1,600 trees), *G. porosum* is in the russuloid clade (nested with *Laxitextum bicolor* and *Dentipellis separans*), but in islands 5 and 7 (totaling 120 trees), this species is in the polyporoid clade (Figs. 1, 2). Consequently, the polyporoid and russuloid clades partially collapse in the strict consensus of all equally parsimonious trees. When *G. porosum* was excluded from the analysis, bootstrap support for the russuloid clade increased to 76% and support for the polyporoid clade rose to 36% (levels of support for the other major clades were not substantially changed; Fig. 1). Several anatomical characters suggest that *G. porosum* is closely related to *L. bicolor* and

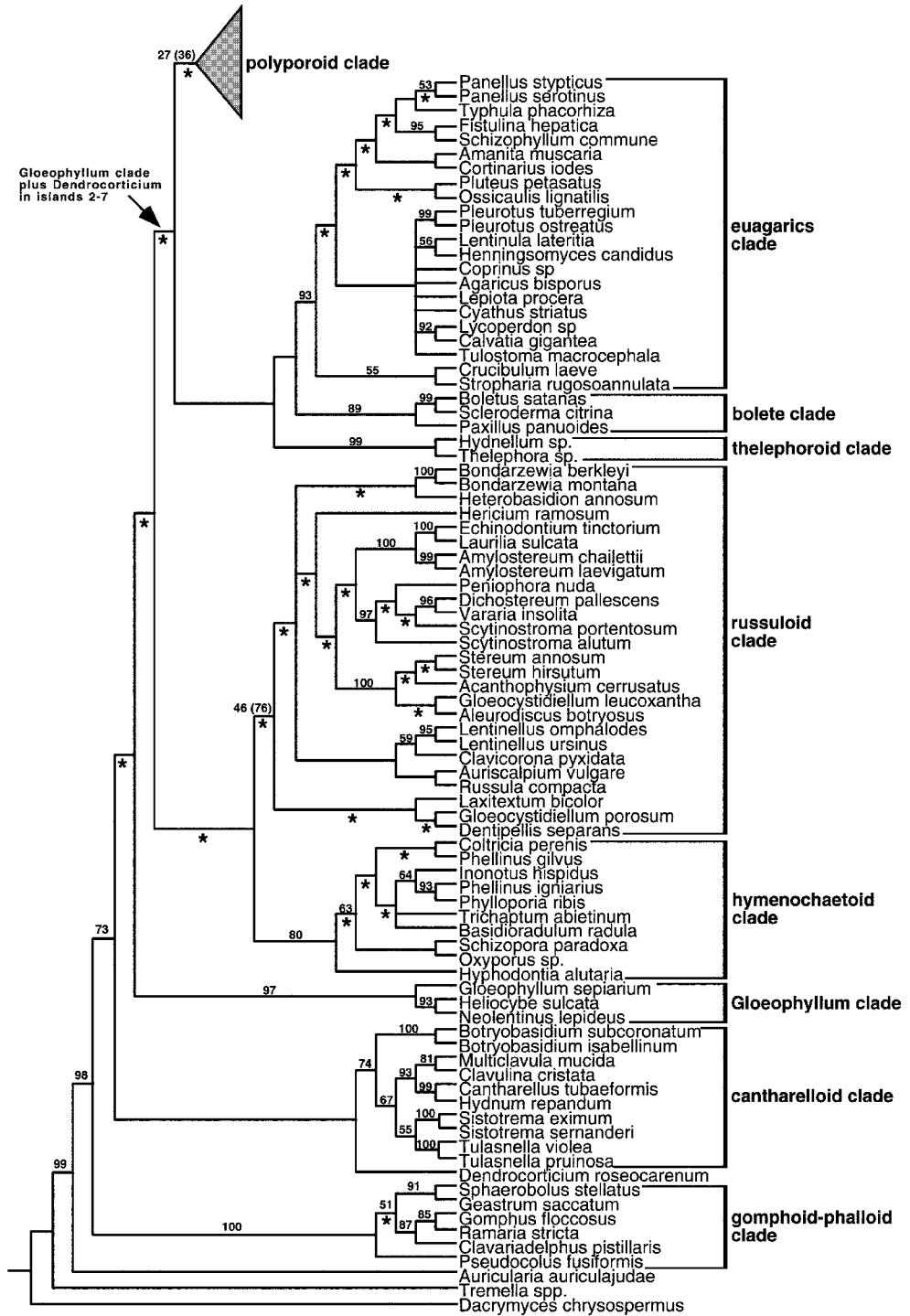


FIGURE 1. Strict consensus of 160 trees (6,421 steps, CI = 0.273, RI = 0.0526) in island 1 of combined analyses of mt-rDNA and nu-rDNA, including all taxa. Numbers above branches are bootstrap frequencies. Bootstrap values <50% are not shown, unless the clade is discussed in the text. The parenthetical bootstrap values for the polyporoid clade (36%) and russuloid clade (76%) are from analyses that exclude *Gloeocystidiellum porosum*. Asterisks indicate nodes that collapse in the strict consensus of all 1,720 equally parsimonious trees. Arrow indicates the position of the *Gloeophyllum* clade plus *D. roseocarenum* in islands 2–7 (1,560 trees). Bracketed groups are discussed in text. The topology of the polyporoid clade is shown in Figure 2.

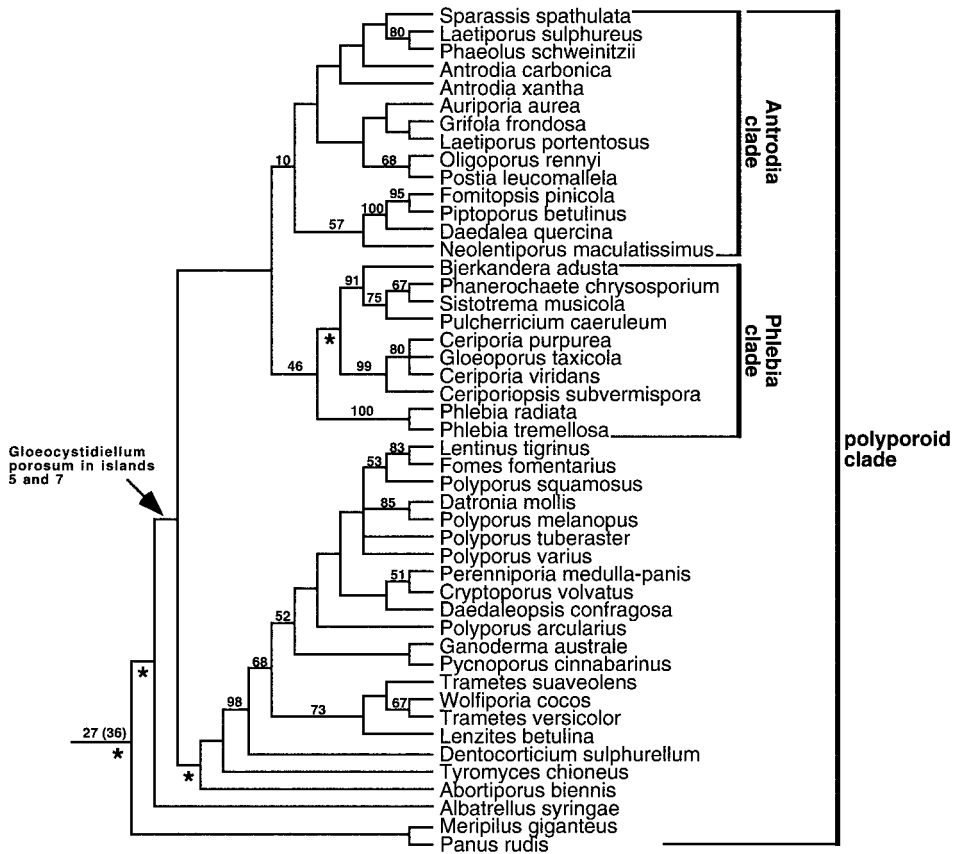


FIGURE 2. Strict consensus of 160 trees (6,421 steps, CI = 0.273, RI = 0.0526) found in island 1 of combined analyses of mt-rDNA and nu-rDNA, including all taxa for the polyporoid clade only. Arrow indicates position of *G. porosum* in islands 5 and 7 (120 trees). The position of the polyporoid clade relative to other taxa is indicated in Figure 1. Other symbols as in Figure 1.

D. separans in the russuloid clade, sharing the presence of "gloeoplerous" hyphae or cystidia (which have an oily, refractive content), amyloid spores (which turn blue in iodine reagent), elliptic spores with minute spines (in *G. porosum* and *L. bicolor* only), a resupinate fruiting body, and a smooth hymenophore (in *G. porosum* and *L. bicolor* only; *D. separans* has a toothed hymenophore). In contrast, no distinctive morphological characters support placement of *G. porosum* in the polyporoid clade. The russuloid clade was supported as monophyletic by the nu-rDNA data alone but not by the mt-rDNA data alone. *Gloeocystidiellum porosum* lacks nu-rDNA. We speculate that the destabilizing effect of including *G. porosum* would be mitigated by including nu-rDNA data for this taxon.

In islands 2–7 (1,560 trees), *Dendrocorticium* is the sister group of the *Gloeophyllum*

clade, and the combined *Dendrocorticium*–*Gloeophyllum* clade is the sister group of the theleporoid, bolete, euagarics, and polyporoid clades (Fig. 1). However, in island 1 (160 trees), *Dendrocorticium* is the sister group of the cantharelloid clade, and the *Gloeophyllum* clade is the sister group of the theleporoid, bolete, euagarics, and polyporoid, hymenochaetoid, and russuloid clades (Fig. 1). As a result, the higher-order relationships among the eight major clades are poorly resolved in the strict consensus of all trees (Fig. 1). Unlike *G. porosum*, the ambiguous placements of *D. roseocarneum* and the *Gloeophyllum* clade cannot be attributed to missing data. All of these species have both nu-rDNA and mt-rDNA sequences, except *Neolentinus lepideus*, which has only nu-rDNA data. Nevertheless, *Neolentinus* is strongly supported as a member of the *Gloeophyllum* clade (as the sister group

of *Heliocybe sulcata*), which is consistent with expectations based on morphology (Pegler, 1983; Redhead and Ginns, 1985), as well as independent analyses of nu-lsu rDNA sequences (Hibbett and Vilgalys, 1993; Thorn et al., 2000).

We had no a priori expectations regarding the placement of *Dendrocorticium*. However, from its morphology, we expected the *Gloeophyllum* clade to be nested in the polyporoid clade, probably closely related to the *Antrodia* clade. This placement was forced under constraint one. Analyses of the full data set under constraint one produced 40 trees of 6,431 steps (10 steps longer than the optimal trees), which we compared with 70 trees that represent the seven islands of unconstrained trees (10 trees from each island). None of the constrained trees could be rejected based on the WSR test ($P = 0.302\text{--}0.355$).

Analyses run under constraint two, which forced monophyly of homobasidiomycetes with perforate parenthesomes, produced 200 trees of 6,423 steps (2 steps longer than the optimal trees), which we tested against the same set of 70 unconstrained trees. None was rejected by the WSR test ($P = 0.854\text{--}0.946$). In summary, taking morphology into account, we interpret the trees from islands 1–4 and 6 (which show *G. porosum* in the rusuloid clade) as the best estimates of the phylogeny. Nevertheless, based solely on molecular characters, trees from the other islands are equally parsimonious, and trees pro-

duced under constraints one and two cannot be rejected.

Character Coding and Ancestral State Reconstructions

Parsimony-based inferences about historical patterns of character state transformations are dependent on the topology of the phylogenetic tree (Donoghue and Ackerly, 1996) and the loss:gain cost ratio that is assumed (Ree and Donoghue, 1998; Swofford and Maddison, 1992). To assess the sensitivity of our results to these factors, we used a range of phylogenetic tree topologies and loss:gain cost ratios to perform ancestral state reconstructions (Table 4). The trees included all 1,720 equally parsimonious trees from the unconstrained combined analysis of the full data set, as well as 240 suboptimal trees from the two constrained analyses. The strict consensus of the most-parsimonious trees is largely unresolved, reflecting the conflicting placements of several taxa (Figs. 1, 2). Nevertheless, most characters had only minor variation across trees in the overall number of losses versus gains inferred at a given loss:gain cost ratio (Table 4). For example, the number of losses and gains in decay mode inferred under a 1:1 loss:gain cost ratio ranged from 1–2 losses and 5–7 gains across all 1,960 trees examined. In contrast, ancestral state reconstructions were often quite sensitive to variation in loss:gain cost ratios. For example, looking at tree 1

TABLE 4. Numbers of losses and gains in decay mode, mating system, and substrate range characters inferred when using different loss:gain cost ratios and tree topologies.

Character / analysis (no. trees)	Inferred losses (1 → 0) / inferred gains (0 → 1) (min–max over all trees) for following loss:gain cost ratios				
	3:1	2:1	1:1	1:2	1:3
Decay mode: 0 = white rot; 1 = brown rot					
Unconstrained (1,720)	1–1/7–7	1–1/7–7	1–2/6–7	2–2/6–6	2–17/1–6
Constraint 1 (40)	1–1/6–6	1–1/6–6	1–2/5–6	2–2/5–5	2–2/2–5
Constraint 2 (200)	1–1/7–7	1–1/7–7	1–2/6–7	2–2/6–6	2–2/6–6
Mating system: 0 = tetrapolar; 1 = bipolar					
Unconstrained (1,720)	0–0/6–6	0–0/6–6	0–0/6–6	0–10/1–6	6–13/1–3
Constraint 1 (40)	0–0/6–6	0–0/6–6	0–1/5–6	1–7/2–5	7–10/1–2
Constraint 2 (200)	0–0/6–6	0–0/6–6	0–0/6–6	0–10/1–6	10–12/1–1
Conifer decay: 0 = unable to decay conifer wood; 1 = able to decay conifer wood					
Unconstrained (1,720)	0–5/35–51	4–8/28–38	12–30/5–24	27–43/0–7	39–43/0–0
Constraint 1 (40)	1–3/40–47	5–7/31–36	19–28/6–15	28–40/0–6	40–40/0–0
Constraint 2 (200)	0–4/37–51	4–8/29–38	18–28/5–16	28–41/0–6	38–41/0–0
Conifer exclusivity: 0 = not limited to conifer decay; 1 = only on conifers					
Unconstrained (1,720)	0–0/12–12	0–0/12–12	0–4/8–12	3–9/6–9	4–10/6–8
Constraint 1 (40)	0–0/11–12	0–0/11–12	0–4/8–12	2–4/8–9	9–21/2–6
Constraint 2 (200)	0–0/12–12	0–0/12–12	0–3/9–12	3–5/8–9	12–12/5–5

from the unconstrained analysis, 1 MPR of wood decay was inferred when using a 3:1 loss:gain cost ratio, indicating 1 loss and 7 gains, but 81 MPRs were inferred when using a 1:3 loss:gain cost ratio, indicating 2–17 losses and 1–6 gains (Table 4). Thus, in this study, inferences about general patterns of character evolution are more sensitive to assumptions about loss:gain bias than to choice among plausible alternative tree topologies. The sensitivity of the ancestral state reconstructions to alternative trees and loss:gain cost ratios (Table 4) provides a measure of their robustness.

Decay mode.—Eighty-nine species (67%) were scored as white rot, and 21 species (16%) were scored as brown rot. All of the taxa that had been scored as missing were optimized by equally weighted parsimony on unconstrained trees as having white rot (total scored plus inferred: 112 species [84%]). Gilbertson (1980) estimated that 7% of North American wood-decaying fungi produce a brown rot. Considering only the saprotrophic or pathogenic species in our data set, 18.3% produce a brown rot, which suggests this character state is overrepresented in our data set.

Ancestral state reconstructions on the unconstrained trees under a 1:1 loss:gain cost ratio have two MPRs, which suggests there have been one to two transformations from brown rot to white rot, and six to seven transformations from white rot to brown rot (Fig. 3; Table 4). The reason for the alternative reconstructions is that *Dacrymyces chrysospermus*, a brown rot species, is one of the basal taxa in the outgroup, and therefore the root node can be resolved as either brown rot or white rot (Fig. 3). Nevertheless, both MPRs suggest that the ancestor of the homobasidiomycetes was a white rot fungus, as was suggested by Gilbertson (1980; contra Nobles, 1965, 1971) (Fig. 4), and that six independent origins of brown rot, have occurred in the lineages leading to *Wolfiporia cocos*, *Fistulina hepatica*, *Ossi-caulis lignatilis*, *Paxillus panuoides*, the *Gloeophyllum* clade (*Gloeophyllum*, *Heliocybe*, and *Neolentinus*), and a weakly supported (bootstrap < 50%) group of 14 species that we call the “*Antrodia* clade” (Figs. 2, 3). This may be an underestimate of the number of gains of brown rot, however, because certain brown rot taxa that we did not sample might represent additional independent origins of

brown rot (e.g., the agaric mushroom *Hypsizygyus*, the corticioid *Veluticeps*, and others) (Gilbertson, 1980).

All MPRs on unconstrained trees under a 1:1 loss:gain cost ratio suggest a reversal from brown rot to white rot in the lineage leading to *Grifola frondosa*, which is nested among 13 brown rot species in the *Antrodia* clade (Fig. 2). To assess the robustness of the hypothesized reversal, we performed additional ancestral state reconstructions on the unconstrained trees, increasing the cost of losses. At a 4:1 loss:gain cost ratio, it becomes equivocal whether the white rot condition of *Grifola* is plesiomorphic or secondarily derived. We also performed an additional constrained analysis of the full data set (using 100 replicate searches in step one of the analysis) that forced *Grifola* to be the sister group of the rest of the *Antrodia* clade. Thirty trees were obtained that are only two steps longer than the unconstrained trees and could not be rejected by the WSR test ($P = 0.904$). Again, whether white rot in *Grifola* is plesiomorphic or derived is equivocal.

Under most loss:gain cost ratios examined, trees produced under constraint 1 (which forces monophyly of the *Gloeophyllum* clade plus the *Antrodia* clade) require one fewer gain of brown rot than the unconstrained trees or the trees produced under constraint 2. Otherwise, the number of losses and gains of brown rot is fairly robust to the choice of tree topology and loss:gain cost ratio.

Our results provide a phylogenetic framework for comparative biochemical studies of wood decay mechanisms. The challenge arising from our results is to test the hypothesis that brown rot evolved repeatedly and to elucidate the genetic basis of transformations between white and brown rot. To do so, we must compare the decay mechanisms of the putatively convergent brown rot clades.

The most obvious chemical difference between brown rot and white rot modes of wood decay is that brown rot fungi do not appreciably degrade lignin, whereas white rot fungi degrade lignin extensively. The lignin-modifying enzymes characterized in white rot fungi include laccases, lignin peroxidases (LIP), and manganese-dependent peroxidases (MNP). Gilbertson (1980) and others have suggested that brown rot fungi lack these enzymes. Nevertheless, a few brown rot fungi do have laccase, LIP, or MNP activity (Szkwarz et al., 1989; Dey et al., 1991;

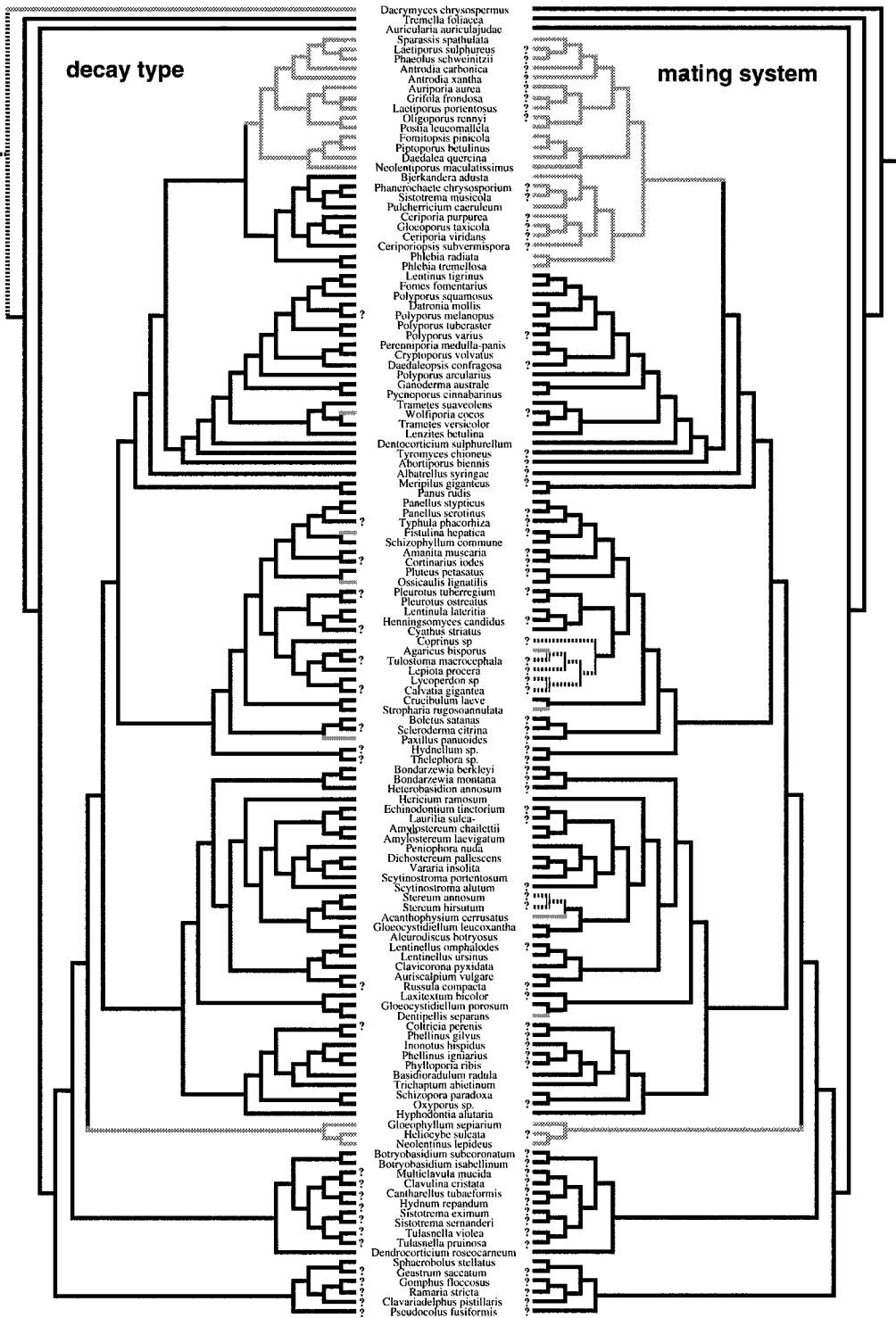


FIGURE 3. Ancestral state reconstructions of decay mode (left, consensus of two MPRs) and mating system (right, consensus of 10 MPRs) on tree 1 from combined analysis of the full data set, inferred with 1:1 loss:gain cost ratio. Decay mode branch shading: black = white rot, gray = brown rot, dashed = equivocal. Mating system branch shading: black = tetrapolar, gray = bipolar, dashed = equivocal. Question marks indicate taxa that could not be scored for the character.

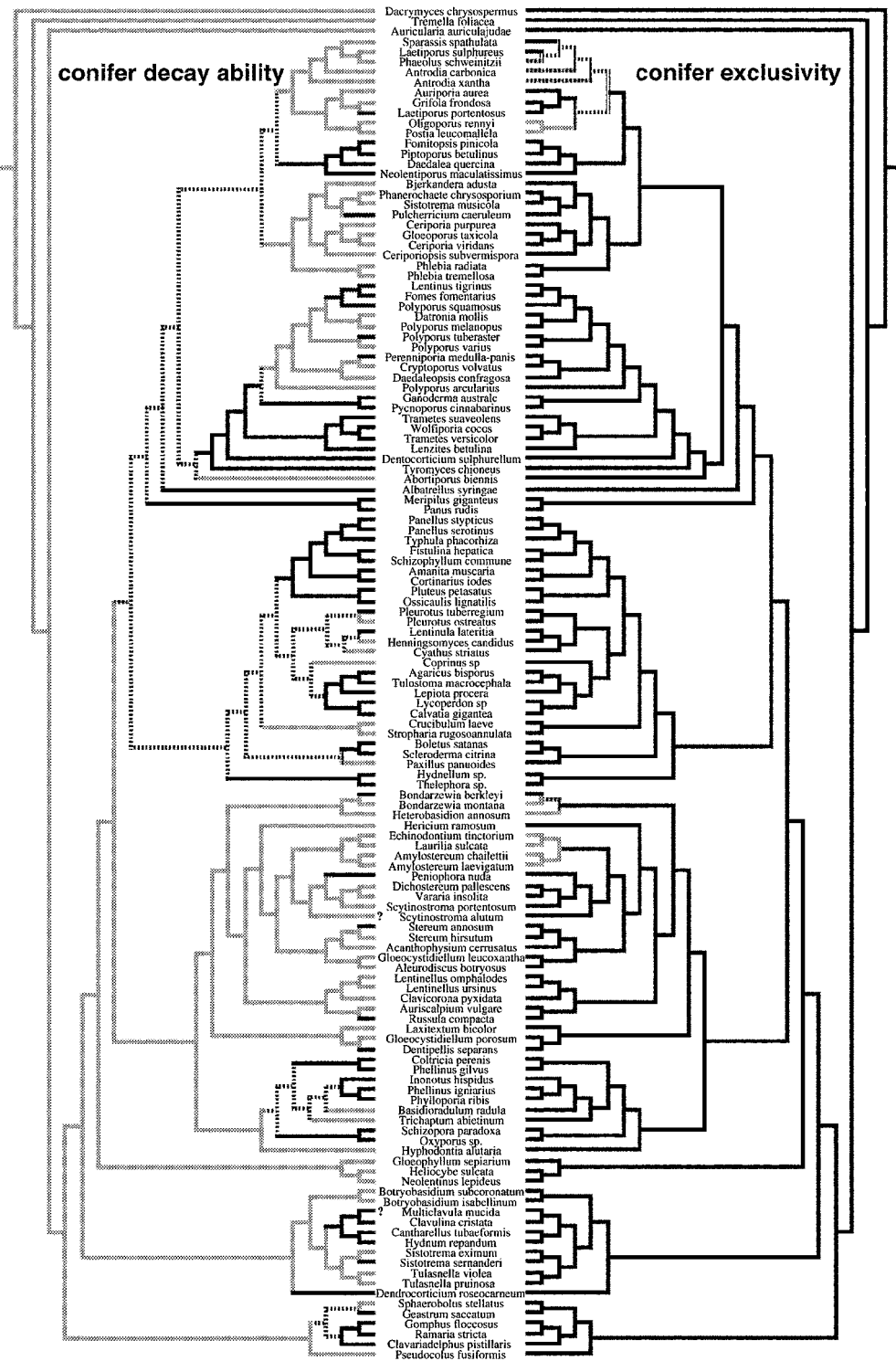


FIGURE 4. Ancestral state reconstructions of conifer decay ability (left, consensus of 264 MPRs) and conifer exclusivity (right, 1 MPR) on tree 1 from combined analysis of the full data set, inferred with 1:1 loss:gain cost ratio. Conifer decay ability branch shading: black = does not decay conifer substrates, gray = decays conifer substrates, dashed = equivocal. Conifer exclusivity branch shading: black = not on or not limited to conifer substrates, gray = found only on conifer substrates, dashed = equivocal. Question marks indicate taxa that could not be scored for the character.

D'Souza et al., 1996; Worrall et al., 1997), and laccase-specific gene sequences in the brown rot fungus *Gloeophyllum trabeum* have been detected by PCR (D'Souza et al., 1996). Unfortunately, few studies have focused on the lignin-modifying enzymes of brown rot fungi and so whether the general features of brown rot fungi include the capacity to degrade lignin (and if so, by which enzymes) is not known.

Another important difference between brown rot and white rot decay mechanisms is the mode of cellulose depolymerization. Almost all white rot fungi that have been tested can degrade pure cellulose in culture, whereas most brown rot fungi lack this ability (Nilsson, 1974). In addition, white rot fungi degrade cellulose by a purely enzymatic mechanism, whereas brown rot fungi initiate cellulose depolymerization by a nonenzymatic oxidative mechanism (Worrall et al., 1997). However, the few brown rot fungi that can degrade pure cellulose in culture apparently have retained the cellulolytic enzyme exo-1,4- β -glucanase (Highley, 1975; Nilsson and Ginns, 1979; Green and Highley, 1997; Worrall et al., 1997). Most of these are members of the bolete clade, in the genera *Coniophora*, *Hygrophoropsis*, *Serpula*, and *Paxillus*, but a few brown rot fungi not in the bolete clade also reportedly can degrade pure cellulose in culture (e.g., *Postia* and *Gloeophyllum* [Nilsson, 1974]).

The evidence discussed above suggests that certain lignin and cellulose-degrading enzyme systems typically associated with white rot have been retained in some groups of brown rot fungi (Worrall et al., 1997). If so, then transformations from white rot to brown rot probably involve changes in the expression patterns of genes for enzymes involved in white rot (as well as gain of the nonenzymatic mechanism of cellulose depolymerization), rather than the absolute loss of those genes. Worrall et al. (1997) noted that in brown rot fungi, lignin degradation (although limited) is most pronounced in late stages of decay whereas in white rot fungi selective delignification is most pronounced in early stages of decay; this supports the view that the evolution of brown rot involves changes in the timing of expression of genes encoding lignin-degrading enzymes.

The apparent retention of genes encoding lignin-modifying enzymes in some groups of brown rot fungi has implications for

the expected loss:gain bias of brown rot. If the genes for lignin-modifying enzymes were lost from the genomes of brown rot fungi, then presumably reversals to white rot would be unlikely. However, if lignin-modifying enzymes were retained in some groups of brown rot fungi, then reversals to white rot might be possible. We inferred that one such reversal may have happened in the case of the white rot fungus *Grifola frondosa*, which may be nested among brown rot fungi in the *Antrodia* clade (Fig. 3). Alternative topologies suggesting that the white rot condition of *Grifola* is plesiomorphic could not be rejected. Nevertheless, several brown rot members of the *Antrodia* clade have been shown to have lignin-degrading activity in culture, including *Oligoporus fragilis* (represented in this study by *O. rennyi*), which shows evidence of "vestigial" extracellular phenoloxidase activity (Worrall et al., 1997:217), and *Piptoporus betulinus*, which has MNP activity in culture (Szklarz et al., 1989). Thus, a reversal to white rot in *Grifola* could have involved shifts in expression patterns of retained lignin-modifying enzymes.

Mating system.—Forty-five species (34%) were scored as tetrapolar and 15 species were scored as bipolar (11%). Equally weighted parsimony optimizations on unconstrained trees optimized as tetrapolar 50–57 of the taxa that had been scored as missing and optimized 16–23 as bipolar (total scored plus inferred: 95–102 species [71–77%] tetrapolar; 31–38 species [23–29%] bipolar). These proportions compare well with figures from Esser (1967), which suggest that ~25% of homobasidiomycetes are bipolar.

At a 1:1 loss:gain cost ratio, 10 MPRs of mating system are found on the unconstrained trees. All 10 MPRs suggest that tetrapolar mating systems are plesiomorphic in the homobasidiomycetes, as suggested by Raper and Flexer (1971; contra Nobles, 1971, Ryvardeen, 1991) (Fig. 3), and six transformations from tetrapolar to bipolar mating systems have taken place, with no reversals (Fig. 3; Table 4). This inference is generally robust at 1:1, 2:1, or 3:1 loss:gain cost ratios on all trees. However, at a 1:1 loss:gain cost ratio, some trees that were produced under constraint one suggest only five transformations from tetrapolar to bipolar mating systems and one reversal (Table 4). At lower loss:gain cost ratios, the inferred number of gains of bipolarity decreases, however, and

at a 1:3 loss:gain cost ratio, all three sets of trees support some MPRs that suggest a single origin of bipolar mating systems, with numerous (6–13) reversals to tetrapolar mating systems (Table 4).

At a 1:1 loss:gain cost ratio, the largest clade of bipolar species is a weakly supported (bootstrap < 50%) group of 24 species in the polyporoid clade, which includes the brown rot *Antrodia* clade and its sister group, a group of 10 white rot species we refer to as the “*Phlebia* clade” (Figs. 2, 3). Mating type has been recorded in just 9 species of the *Antrodia* clade and *Phlebia* clade; the states in the remaining 15 taxa have been inferred from the equally weighted parsimony optimization (Fig. 3).

The view that tetrapolarity is plesiomorphic in the homobasidiomycetes (Raper and Flexer, 1971) is supported by the fact that the heterobasidiomycete Auriculariales, which is supported as the sister group of the homobasidiomycetes, is tetrapolar (Figs. 1, 3). However, our ancestral state reconstructions may grossly underestimate the number of transformations in mating type that have taken place within the homobasidiomycetes because 73 species (55%) could not be scored for mating system. With so many missing data, parsimony optimizations could easily have underestimated the actual number of transformations. Moreover, the distribution of bipolar and tetrapolar mating systems among some putatively closely related species of homobasidiomycetes suggests that mating systems are fairly labile. For example, the genera *Sistotrema*, *Marasmius*, *Collybia*, and *Coprinus* each contain both tetrapolar and bipolar species (Lange, 1952; Raper and Flexer, 1971; Murphy and Miller, 1993; Petersen, 1995). To obtain more realistic estimates of the number of transformations in mating systems, one will need to obtain more baseline data on mating systems in homobasidiomycetes and perform ancestral state reconstructions by using more comprehensive phylogenetic trees of homobasidiomycetes than those in the present study.

As with decay mode, our results provide a phylogenetic framework for studying the genetic basis of transformations between mating systems. Theoretical and empirical studies suggest that switches from tetrapolar to bipolar mating systems could occur by at least two mechanisms: (1) “self-compatible” mutations at either the A or B mating type loci

of tetrapolar mating systems could create effectively bipolar mating systems (Raper and Flexer, 1971; Casselton and Kües, 1994), and (2) chromosome rearrangements that bring A and B loci into tight linkage groups could convert tetrapolar mating systems to bipolar mating systems (Bakkeren et al., 1992). Studies on the genetic architecture of the putatively independently derived bipolar mating systems could help refine hypotheses of homology in this character.

Conifer decay ability.—Fifty-seven species were scored as unable to decay conifer wood, and 74 species were scored as able to decay conifer wood (such taxa may or may not decay other substrates). Ancestral state reconstructions of conifer decay ability are ambiguous. At a 1:1 loss:gain cost ratio, tree 1 from the unconstrained analysis has 264 MPRs, suggesting 12–30 losses of conifer decay ability, and 5–24 gains (Fig. 4). Nevertheless, all MPRs suggest that the plesiomorphic condition of the homobasidiomycetes is to possess the ability to decay conifers (Fig. 4).

Conifer exclusivity.—Conifer exclusivity has a much more limited distribution than conifer decay ability. We scored 116 species as not occurring exclusively on conifers and 16 species as occurring exclusively on conifers. The ancestral condition of the homobasidiomycetes is to lack conifer exclusivity. At a 1:1 loss:gain cost ratio, the three sets of trees suggest 0–4 losses of conifer exclusivity and 8–12 gains (Fig. 4; Table 4). At loss:gain cost ratios of 3:1 or 2:1, all trees suggest 11–12 gains of conifer exclusivity and no reversals. At lower loss:gain cost ratios, however, the number of inferred losses increased, and at a 1:3 loss:gain cost ratio, 4–21 losses and 2–8 gains were inferred (Table 4). Together, the parsimony optimizations of conifer decay ability and conifer exclusivity suggest that the plesiomorphic condition of the homobasidiomycetes is to be a generalist, able to decay conifers and other substrates, although scattered shifts to a specialization for conifer substrates have occurred. However, the precise number of such shifts (and possible reversals) is sensitive to the assumed loss:gain cost ratio.

Correlation Analyses

We used the CCT to evaluate potential correlations between decay mode, mating

TABLE 5. Results of concentrated changes test for equally weighted parsimony optimizations on tree 1, island 1.

Independent character		Dependent character					
Character and "distinguishing state"	MPR	Character and derived state	MPR	Total gains	Total losses	Gains in "distinguished clades"	<i>P</i> ^c
Decay mode/brown rot	1/2 ^a	Conifer exclusivity /yes	1/10	12	0	5–6 ^b	0.022–0.011
			10/10	8	4	2–3 ^b	NS
Mating system/bipolar	1/1	Mating system/bipolar	1/1	6	0	0–1 ^b	NS
			1/10	12	0	5	NS
		Conifer exclusivity /yes	10/10	8	4	2	NS
			1/2	6	2	1–2 ^b	NS
		Decay mode/brown rot	2/2	7	1	1–2 ^b	NS

^aAnalyses with decay mode as the independent character used only MPR1 because the alternative MPR differs only in the resolution of the root node (see Fig. 3).

^bVariation is due to alternative interpretations of characters that change on the same branch.

^cCorrected for multiple tests. NS, not significant.

system, and conifer exclusivity. However, we decided not to perform any CCTs for the alternative substrate range character, conifer decay ability. All 264 MPRs of conifer decay ability suggested that the capacity to decay conifer wood is a widespread plesiomorphic character in the homobasidiomycetes. Therefore, we felt it unlikely that evidence would suggest the ability to decay conifers is either a cause or consequence of the evolution of brown rot or bipolar mating systems, both of which appear to be highly derived conditions. In addition, the ambiguous ancestral state reconstruction of conifer decay ability (Fig. 4) would make it difficult to use this character in the CCT.

No changes in decay mode or mating system were inferred to have occurred within clades that are distinguished by having conifer exclusivity. Therefore, we investigated possible causal relationships involving the following pairs of characters (the first character listed being the putatively independent character): (1) decay mode versus conifer exclusivity; (2) decay mode versus mating system; (3) mating system versus conifer exclusivity; and (4) mating system versus decay mode (Table 5). We performed the CCT under different MPRs and assumptions regarding the sequence of changes in branches where both characters were inferred to have changed (Table 5). In total, 11 CCTs were performed. Therefore, all *P* values were multiplied by 11 to correct for multiple tests.

Three of the correlations were found to be nonsignificant, including that between evolution of a brown rot and evolution of bipo-

lar mating systems. Without considering the phylogeny, this result was somewhat surprising because 16 of 20 brown rot species in our dataset were scored as having bipolar mating systems. However, ancestral state reconstructions suggest that the bipolar brown rot species represent just two independent clades (Fig. 3). The larger of the two is the *Antrodia* clade, which includes 13 species (and is weakly supported as the sister group of the bipolar white rot *Phlebia* clade). The remaining bipolar brown rot species are in the *Gloeophyllum* clade. Depending on the interpretation of simultaneous changes in decay mode and mating system on the branch leading to the *Gloeophyllum* clade, only one or two derivations of brown rot are localized within bipolar clades, which is not significantly different from a pattern of association that could be expected by chance (Table 5). These results illustrate the danger of inferring causal relationships among characters in an ahistorical framework.

The only character comparison that returned a significant correlation was decay mode versus conifer exclusivity, but this was sensitive to the choice of MPR of conifer exclusivity (Table 5). Ten MPRs of conifer exclusivity were inferred by using equally weighted parsimony optimizations, requiring 8–12 gains and 0–4 losses. In addition, simultaneous gains in conifer exclusivity and decay mode were inferred on the branch leading to *Paxillus panuoides*. Under MPR1 of conifer exclusivity (0 losses, 12 gains), 5–6 gains could be localized within brown rot clades, depending on how the simultaneous changes on the branch leading to

TABLE 6. Results of concentrated changes test for correlation between conifer exclusivity (dependent character) and decay mode on alternative topologies.

Tree	MPR of conifer exclusivity	Total gains	Total losses	Gains in brown rot clades ^a	<i>P</i> (uncorrected)
Island 2, tree 1	MPR 1/5	12	0	5–6	0.007–0.002
	MPR 5/5	9	3	2–3	0.295–0.081
Island 3, tree 1	MPR 1/5	12	0	5–6	0.011–0.000
	MPR 5/5	9	3	2–3	0.289–0.070
Island 4, tree 1	MPR 1/10	12	0	5–6	0.012–0.001
	MPR 10/10	8	4	2–3	0.231–0.047
Island 5, tree 1	MPR 1/5	12	0	5–6	0.013–0.001
	MPR 5/5	9	3	2–3	0.267–0.073
Island 6, tree 1	MPR 1/10	12	0	5–6	0.016–0.003
	MPR 10/10	8	4	2–3	0.216–0.056
Island 7, tree 1	MPR 1/5	12	0	5–6	0.018–0.001
	MPR 5/5	9	3	2–3	0.260–0.057
Constraint 1, tree 1	MPR 1/8	12	0	5–6	0.010–0.001
	MPR 8/8	8	4	2–3	0.289–0.069
Constraint 2, tree 1	MPR 1/5	12	0	5–6	0.008–0.001
	MPR 5/5	9	3	2–3	0.300–0.065

^aVariation is due to alternative resolutions of simultaneous changes in conifer exclusivity and decay mode on branch leading to *Paxillus panuoides*.

Paxillus were interpreted. This correlation was deemed significant by the CCT ($P = 0.022$ if five gains of conifer exclusivity are inferred in brown rot clades; $P = 0.011$ if six gains are inferred). However, under MPR10 of conifer exclusivity (four losses, eight gains), only two to three gains were inferred within brown rot clades, which was not significant after correcting for multiple tests.

To explore the sensitivity of the correlation between decay mode and conifer exclusivity to alternative tree topologies, we performed the CCT by using one tree from each of the remaining six islands discovered in the unconstrained analysis, as well as one tree from each of the two constrained analyses (Table 6). There were 5–10 MPRs of conifer exclusivity on the eight trees examined. In every tree, the MPR of conifer exclusivity that maximized gains showed five to six gains of conifer exclusivity in brown rot clades, which was significant ($P = 0.001$ – 0.018 ; uncorrected P values), whereas the MPR that maximized losses had two to three such gains, which was only marginally significant or nonsignificant ($P = 0.047$ – 0.300 ; uncorrected P values; Table 6).

As a complement to the CCT, we used the ML test in Discrete to evaluate the correlation between brown rot and conifer exclusivity that was suggested by (some) CCTs. The best-fit model with nine free parameters had $-\log L(D_9) = 71.936$, whereas the best-fit model with eight free parameters

had $-\log L(D_8) = 74.069$. The likelihood ratio statistic for the best-fit models from each class is 4.266, which is significant ($0.05 > P > 0.025$). In the optimal nine-parameter model, the rate parameter specifying the probability of a shift to conifer substrates when the background condition is white rot is 0.018, whereas when the background condition is brown rot the rate parameter is 0.163. These results suggest that the instantaneous probability of a shift to conifer exclusivity is approximately nine times greater in brown rot clades than in white rot clades.

The hypothesis of a causal relationship between brown rot and conifer exclusivity was supported by both the CCT and the ML method implemented in Discrete (Tables 4–6). Although these two methods supported similar conclusions, they evaluate character correlations by very different approaches. In the CCT, the test of character correlation is based on fully resolved ancestral state reconstructions for each of the characters of interest. This is problematic for two reasons: (1) the ancestral state reconstructions depend on assumed loss:gain cost ratios, which must be specified a priori; and (2) there are often multiple MPRs for each character, which increases the number of tests that must be performed (simultaneous inferred changes exacerbate this problem [Maddison, 1990]). These problems were manifested in our study: Under the CCT, conclusions regarding the correlation between brown rot

and conifer exclusivity were sensitive to the choice among MPRs and the interpretation of simultaneous changes (Tables 4, 5). Moreover, the ancestral state reconstructions that formed the basis of the CCT were often sensitive to variation in loss:gain cost ratios (Table 4). Considering all this, the results of the CCT are rather ambiguous.

In contrast to the CCT, the ML method in Discrete estimates the probabilities of character state transformations directly from the hypothesized phylogeny and the states of the terminal taxa. In addition, the likelihood scores used to evaluate competing models of evolution are calculated over all possible combinations of ancestral states. Thus, the ML method does not involve as many assumptions about evolutionary history and process as the CCT. Nevertheless, certain sources of error affect both methods, including error in the estimation of the phylogenetic tree itself (Donoghue and Ackerly, 1996). We assessed the sensitivity of our results to alternative tree topologies by performing the CCT over a range of equally parsimonious trees (picking trees from different islands in an attempt to maximize topological disparity) as well as two suboptimal trees that could not be rejected by the WSR test (Table 6). All trees yielded similar results, including sensitivity to the choice of MPRs.

The results of our sensitivity analyses recall those of Donoghue and Ackerly (1996), who studied correlations in simulated and empirical characters on a range of equally parsimonious trees, suboptimal trees, and random trees. Overall, these authors found that conclusions regarding character correlations were generally robust to choices among equally parsimonious or marginally suboptimal trees, but inferences based on random trees were no more reliable than those that did not take phylogeny into account at all. Their results, and ours in the present study, suggest that causal interactions among characters may often be detectable across a range of plausible trees, which is encouraging for comparative studies of large taxonomic groups. However, this may not be true in all cases, so topological sensitivity analyses should be a routine component of comparative studies. In particular, trees that imply alternative patterns of evolution in the focal characters should be investigated. For example, in this study we examined subop-

timal trees that force the monophyly of the *Antrodia* clade and the *Gloeophyllum* clade, both of which include brown rot species. The constrained trees that show the *Antrodia* clade and the *Gloeophyllum* clade to be monophyletic imply one fewer gain of brown rot than the optimal trees (Table 4). Nevertheless, the correlation between brown rot and conifer exclusivity was upheld on this topology (again, depending on the choice of MPRs).

Another potential source of error in comparative analyses is incomplete or biased taxon sampling (Maddison, 1990; Sillén-Tullberg, 1993; Höglund and Sillén-Tullberg, 1994; Werdelin and Tullberg, 1995; Donoghue and Ackerly, 1996; Hillis, 1998; Lorch and Eadie, 1999; Ree and Donoghue, 1999). For example, Sillén-Tullberg (1993) and Höglund and Sillén-Tullberg (1994) described cases in which conclusions based on the CCT were overturned based on a repeat application of the test with an increased sample of taxa. Similarly, Ree and Donoghue (1999) found that ML estimates of transformation probabilities may be quite sensitive to taxon sampling. Ree and Donoghue estimated the rate of gains versus losses of zygomorphic (bilaterally symmetric) flowers in angiosperms by using Discrete. With an initial sample of 379 species, asymmetry in the rate of losses versus gains was significant (favoring losses), but when the number of zygomorphic species was doubled, to better reflect the actual proportion of described zygomorphic species, the asymmetry became nonsignificant. A general implication of these studies is that comparative analyses of character evolution should be based on samples of taxa that reflect, as nearly as possible, the actual phylogenetic distribution of species and character states.

Our data set included a diverse, fairly comprehensive sampling of homobasidiomycetes. Nevertheless, sampling bias is evident in the distribution of taxa as well as character states. Overrepresented categories include the polyporoid clade and brown rot species, whereas underrepresented categories include the euagarics clade (Table 3). We will continue to add taxa to our data set, with the goal of making the sampling of clades and character states more representative of the actual proportions. In the meantime, given our current best estimates of the phylogeny (Figs. 1, 2), we conclude

that the repeated evolution of brown rot has promoted repeated shifts to conifer exclusivity in homobasidiomycetes (Tables 4–6).

Two hypotheses have been proposed to explain the apparent correlation between brown rot and decay of conifer substrates. Gilbertson (1980) suggested that brown rot and conifer decay are correlated because the short growing seasons and other environmental factors of conifer-dominated forests favor brown rot fungi. A corollary of Gilbertson's (1980) hypothesis is that the frequency of brown rot fungi should increase on all substrate types in conifer-dominated forests, not just on conifer wood. However, studies in the boreal forests of Lapland (Renvall et al., 1991) and Northern Québec (Niemelä, 1985) suggest that even in these extreme, conifer-dominated environments, brown rot fungi show a preference for conifer substrates. Specifically, Renvall et al. (1991) found that 15 (75%) of 20 brown rot species were exclusively found on conifers, compared with 26 (49%) of 53 white rot species, and Niemelä (1985) found that 9 (82%) of 11 brown rot species were exclusively found on conifers, compared with 9 (45%) of 20 white rot species. These observations suggest that the correlation between brown rot and decay of conifer substrates cannot be explained solely by environmental factors.

An alternative explanation for the correlation between brown rot and decay of conifer substrates was proposed by Rayner and Boddy (1988), who suggested that brown rot fungi, which do not extensively decay lignin, are most prevalent on conifer wood because the lignins of conifers are more resistant to decay than the lignins of hardwoods. If some physical or chemical property of conifer wood enhances the growth or competitive ability of brown rot fungi, then quantitative measures of decay (e.g., substrate weight loss [Worrall et al., 1997]) may be useful for detecting differences in the relative abilities of brown rot and white rot fungi to decay hardwood versus conifer substrates. With appropriate taxonomic sampling, empirical data from laboratory decay studies could be used in phylogenetic comparative analyses to test whether shifts in decay abilities correlate with transformations between decay modes. For example, one could use the ML method of Pagel (in Lutzoni and Pagel, 1997), which allows comparisons of continuous characters (e.g., de-

decay ability) and discrete characters (e.g., decay mode). If such analyses suggested that brown rot confers a performance advantage on conifer substrates, then further mechanistic studies would be warranted to elucidate the biochemical basis of the correlation between brown rot and conifer exclusivity.

Conclusions

Our study inferred historical patterns of evolution in decay mode, mating type, and substrate range characters and assessed prior hypotheses of causal relationships among them. Earlier attempts to address these issues have been handicapped by the lack of phylogenetic hypotheses of the homobasidiomycetes. The ancestral condition of decay mode and mating type have been especially controversial (Nobles, 1965, 1971; Raper and Flexer, 1971; Gilbertson, 1980; Watling, 1982; Ryvarden, 1991). Our findings suggest that the ancestor of the homobasidiomycetes was a white rot, tetrapolar fungus, and that brown rot and bipolarity have evolved repeatedly. The ability to decay conifer substrates is plesiomorphic and widespread in the homobasidiomycetes, but conifer exclusivity is a specialized, derived condition.

Gilbertson (1980) noted that a disproportional number of fungi that produce a brown rot grow on conifer wood and have bipolar mating systems. Consequently, he inferred that there is a causal relationship among these characters. We decomposed Gilbertson's hypothesis into three pairwise character comparisons. Two of the comparisons, brown rot versus bipolarity and conifer exclusivity versus bipolarity, yielded non-significant correlations. Thus, our results do not support the view that the evolution of bipolar mating systems is either a cause or a consequence of the evolution of brown rot or conifer exclusivity. Previous conclusions about causal factors in the evolution of bipolar mating systems appear to be in error because they were based on an ahistorical approach that implicitly treats the character states of different species as independent (Gilbertson, 1980).

The only significant correlation we found is that between brown rot and conifer exclusivity. Gilbertson (1980) predicted these characters should be correlated but did not specify the relative timing of the origin of brown

rot and the colonization of conifers. Our results suggest that the evolution of brown rot has often preceded the evolution of conifer exclusivity. However, conifer exclusivity has also evolved at least five or six times within white rot clades (Figs. 3, 4, Tables 3, 4). Apparently, brown rot confers a greater tendency toward shifts to conifer exclusivity than does white rot, but it is not essential for conifer exclusivity.

ACKNOWLEDGMENTS

We thank Mark Pagel for providing a copy of Discrete and advice about its use, Rick Ree for helping to translate trees into Discrete format, the individuals and institutions listed in Table 2 for supplying isolates and DNA samples, Dick Olmstead and an anonymous reviewer for commenting on earlier versions of the manuscript, and the National Science Foundation, for supporting the research (DEB-9629427).

REFERENCES

- BAKKEREN, G., B. GIBBARD, A. YEE, E. FROELINGER, S. LEONG, AND J. KRONSTAD. 1992. The *a* and *b* loci of *Ustilago maydis* hybridize to DNAs from other smut fungi. *Mol. Plant Microbe Interact.* 5:347–355.
- BLANCHETTE, R. A. 1991. Delignification by wood-decay fungi. *Annu. Rev. Phytopathol.* 29:381–398.
- BREITENBACH, J., AND F. KRÄNZLIN. 1995. Fungi of Switzerland, volume 4. Agarics, 2nd part. *Mykologia Lucerne*, Lucerne.
- BRODIE, H. J. 1975. The bird's nest fungi. Univ. of Toronto Press, Toronto.
- BRUNS, T. D., AND T. M. SZARO. 1992. Rate and mode differences between nuclear and mitochondrial small-subunit rRNA genes in mushrooms. *Mol. Biol. Evol.* 9:836–855.
- BRUNS, T. D., R. VILGALYS, S. M. BARNES, D. GONZALEZ, D. S. HIBBETT, D. S. LANE, L. SIMON, S. STICKEL, T. M. SZARO, W. G. WEISBURG, AND M. L. SOGIN. 1992. Evolutionary relationships within the fungi: analysis of nuclear small subunit rRNA sequences. *Mol. Phyl. Evol.* 1:231–242.
- BULL, J. J., J. P. HULSENBECK, C. W. CUNNINGHAM, D. L. SWOFFORD, AND P. J. WADELL. 1993. Partitioning and combining data in phylogenetic analysis. *Syst. Biol.* 42:384–397.
- BURDSALL, H. H., AND O. K. MILLER. 1975. A reevaluation of *Panellus* and *Dictyopanus* Agaricales. *Beih. Nova Hedwigia* 51:79–91.
- CASSELTON, L. A., AND U. KÜES. 1994. Mating-type genes in homobasidiomycetes. Pages 307–321 in *The Mycota*, volume 1. Growth, differentiation, and sexuality (J. G. H. Wessels and F. Meinhardt, eds.). Springer-Verlag, Berlin.
- COKER, W. C., AND J. N. COUCH. 1928. The Gasteromycetes of the eastern United States and Canada. Univ. of North Carolina Press, Chapel Hill.
- CUNNINGHAM, C. W. 1997. Can three incongruence tests predict when data should be combined? *Mol. Biol. Evol.* 14:733–740.
- DE QUEIROZ, A., M. J. DONOGHUE, AND J. KIM. 1995. Separate vs. combined analysis of phylogenetic evidence. *Annu. Rev. Ecol. Syst.* 26:657–681.
- DEY, S., T. K. MAITI, AND B. C. BHATTACHARYA. 1991. Lignin peroxidase production by a brown-rot fungus *Polyporus ostreiformis*. *J. Ferment. Bioeng.* 72:402–404.
- DONK, M. A. 1964. A conspectus of the families of the Aphyllophorales. *Persoonia* 3:199–324.
- DONOGHUE, M. J. 1989. Phylogenies and the analysis of evolutionary sequences, with examples from seed plants. *Evolution* 43:1137–1156.
- DONOGHUE, M. J., AND D. ACKERLY. 1996. Phylogenetic uncertainty and sensitivity analyses in comparative biology. *Philos. Trans. R. Soc. London B* 351:1241–1249.
- DRING, D. M. 1973. Gasteromycetes. Pages 451–478 in *The fungi, an advanced treatise*, volume 4 B (G. C. Ainsworth, F. K. Sparrow, and A. S. Sussman, eds.). Academic Press, New York.
- D'SOUZA, T. M., K. BOOMINATHAN, AND C. A. REDDY. 1996. Isolation of lacase gene-specific sequences from white rot and brown rot fungi by PCR. *Appl. Environ. Microbiol.* 62:3739–3744.
- ERIKSSON, J., K. HJORTSTAM, AND L. RYVARDEN. 1981. The Corticiaceae of North Europe, volume 6. *Phlebia-Sarcodontia*. Fungiflora, Oslo.
- ERIKSSON, J., K. HJORTSTAM, AND L. RYVARDEN. 1984. The Corticiaceae of North Europe, volume 7. *Schizopora-Suillosporium*. Fungiflora, Oslo.
- ESSER, K. 1967. Die Verbreitung der Incompatibilität bei Thallophyten. *Handb. Pflanzenphysiol.* 18:321–343.
- ESSER, K., AND R. BLAICH. 1994. Heterogenic incompatibility in fungi. Pages 211–232 in *The Mycota*, volume 1. Growth, differentiation, and sexuality (J. G. H. Wessels and F. Meinhardt, eds.). Springer-Verlag, Berlin.
- FARRIS, J. S., M. KÄLLERSJÖ, A. G. KLUGE, AND C. BULT. 1994. Testing significance of incongruence. *Cladistics* 10:315–319.
- FARRIS, J. S., M. KÄLLERSJÖ, A. G. KLUGE, AND C. BULT. 1995. Constructing a significance test for incongruence. *Syst. Biol.* 44:570–572.
- FELSENSTEIN, J. 1985. Confidence limits on phylogenies: An approach using the bootstrap. *Evolution* 39:783–791.
- GARGAS, A., P. T. DEPRIEST, M. GRUBE, AND A. TEHLER. 1995. Multiple origins of lichen symbioses in fungi suggested by *ssu* rDNA phylogeny. *Science* 268:1492–1495.
- GILBERTSON, R. L. 1980. Wood-rotting fungi of North America. *Mycologia* 72:1–49.
- GILBERTSON, R. L. 1981. North American wood-rotting fungi that cause brown rots. *Mycotaxon* 12:372–416.
- GILBERTSON, R. L., AND L. RYVARDEN. 1986. North American polypores, volume 1. Fungiflora, Oslo.
- GILBERTSON, R. L., AND L. RYVARDEN. 1987. North American polypores, volume 2. Fungiflora, Oslo.
- GINNS, J. 1997. The taxonomy and distribution of rare or uncommon species of *Albatrellus* in western North America. *Can. J. Bot.* 75:261–273.
- GINNS, J., AND M. N. L. LEFEBVRE. 1993. Lignicolous corticioid fungi (Basidiomycota) of North America: Systematics, distribution, and ecology. *Mycol. Mem.* 19:1–247.
- GRAY, M. W., D. SANKOFF, AND R. J. CEDERGREN. 1984. On the evolutionary descent of organisms and organelles: A global phylogeny based on a highly conserved structural core on small subunit ribosomal RNA. *Nucleic Acids Res.* 12:5837–5852.

- GREEN, F., AND T. L. HIGHLEY. 1997. Mechanism of brown-rot decay: Paradigm or paradox? *Int. Biodet. Biodegrad.* 39:113–124.
- HAWKSWORTH, D. L., P. M. KIRK, B. C. SUTTON, AND D. N. PEGLER. 1995. Dictionary of the fungi, 8th ed. CAB International, Wallingford, U.K.
- HIBBETT, D. S. 1996. Phylogenetic evidence for horizontal transmission of group I introns in the nuclear ribosomal DNA of mushroom-forming fungi. *Mol. Biol. Evol.* 13:903–917.
- HIBBETT, D. S., AND M. J. DONOGHUE. 1995. Progress toward a phylogenetic classification of the Polyporaceae through parsimony analyses of mitochondrial ribosomal DNA sequences. *Can. J. Bot.* 73 (Suppl.):s853–s861.
- HIBBETT, D. S., E. M. PINE, E. LANGER, G. LANGER, AND M. J. DONOGHUE. 1997. Evolution of gilled mushrooms and puffballs inferred from ribosomal DNA sequences. *Proc. Natl. Acad. Sci. USA* 94:12002–12006.
- HIBBETT, D. S., AND R. G. THORN. 2001. Basidiomycota: Homobasidiomycetes. Pages 121–168 in *The Mycota*, volume 7. Systematics and evolution (D. J. McLaughlin, E. G. McLaughlin, and P. A. Lemke, eds.). Springer-Verlag, Berlin.
- HIBBETT, D. S., A. TSUNEDA, AND S. MURAKAMI. 1994. The sectoid form of *Lentinus tigrinus*: Genetics and development of a fungal morphological innovation. *Am. J. Bot.* 81:466–478.
- HIBBETT, D. S., AND R. VILGALYS. 1993. Phylogenetic relationships of *Lentinus* (Basidiomycotina) inferred from molecular and morphological characters. *Syst. Bot.* 18:409–433.
- HIGHLEY, T. L. 1975. Properties of cellulases of two brown-rot fungi and two white-rot fungi. *Wood Fiber* 6:275–281.
- HILLIS, D. M. 1998. Taxonomic sampling, phylogenetic accuracy, and investigator bias. *Syst. Biol.* 47: 3–8.
- HINKLE, G., J. K. WETTERER, T. R. SCHULTZ, AND M. L. SOGIN. 1994. Phylogeny of the attine ant fungi based on analysis of small subunit ribosomal RNA gene sequences. *Science* 266:1695–1697.
- HÖGLUND, J., AND B. SILLÉN-TULLBERG. 1994. Does lekking promote the evolution of male-biased size dimorphism in birds? On the use of comparative approaches. *Am. Nat.* 144:881–889.
- JÜLICH, W., AND J. STALPERS. 1980. The resupinate nonporoid Aphyllophorales of the temperate northern hemisphere. North Holland Publishing, Amsterdam.
- KERRIGAN, R. W., AND I. K. ROSS. 1988. Extracellular lacases: Biochemical markers for *Agaricus* systematics. *Mycologia* 80:689–695.
- LANGE, M. 1952. Species concept in the genus *Coprinus*. *Dansk Bot. Ark.* 14:1–164.
- LARSEN, M. J., AND R. L. GILBERTSON. 1977. Studies in *Laeticorticium* (Aphyllophorales, Corticiaceae) and related genera. *Norw. J. Bot.* 24:99–121.
- LORCH, P. D., AND J. MCA. EADIE. 1999. Power of the concentrated changes test for correlated evolution. *Syst. Biol.* 48:170–191.
- LOWE, J. L. 1966. Polyporaceae of North America. The genus *Poria*. Tech. Publ. State Univ. Coll. For. Syracuse 90:1–183.
- LUTZONI, F. M., AND M. PAGEL. 1997. Accelerated evolution as a consequence of transitions to mutualism. *Proc. Natl. Acad. Sci. USA* 94:11422–11427.
- MADDISON, D. R. 1991. The discovery and importance of multiple islands of most-parsimonious trees. *Syst. Zool.* 40:315–328.
- MADDISON, D. R., M. RUVOLO, AND D. L. SWOFFORD. 1992. Geographic origins of human mitochondrial DNA: Phylogenetic evidence from control region sequences. *Syst. Biol.* 41:111–124.
- MADDISON, W. P. 1990. A method for testing the correlated evolution of two binary characters: Are gains and losses concentrated on certain branches of a phylogenetic tree? *Evolution* 44: 539–557.
- MADDISON, W. P., AND D. R. MADDISON. 1992. MacClade version 3. Sinauer Associates, Sunderland, Massachusetts.
- MARTIN, K. J., AND R. L. GILBERTSON. 1976. The mating system and some other cultural aspects of *Veluticeps berkeleyi*. *Mycologia* 65:548–557.
- MILLER, O. K. 1971. The relationship of cultural characters to the taxonomy of the agarics. Pages 197–216 in *Evolution in the higher basidiomycetes* (R. H. Petersen, ed.). Univ. of Tennessee Press, Knoxville.
- MILLER, O. K., AND L. STEWART. 1971. The genus *Lentinellus*. *Mycologia* 63:333–369.
- MURPHY, J. F., AND O. K. MILLER. 1993. Diversity and local distribution of mating alleles in *Marasmiellus praecutus* and *Collybia subnuda* (Basidiomycetes, Agaricales). *Can. J. Bot.* 75:8–17.
- NAKASONE, K. K. 1990. Cultural studies and identification of wood-inhabiting Corticiaceae and selected Hymenomycetes from North America. *Mycol. Mem.* 15:1–412.
- NIEMELÄ, T. 1985. Mycoflora of Poste-de-la-Baleine, Northern Québec. Polypores and the Hymenochaetales. *Nat. Can. (Rev. Écol. Syst.)* 112:445–472.
- NILSSON, T. 1974. Comparative study on the cellulolytic activity of white-rot and brown-rot fungi. *Mater. Org.* 9:173–198.
- NILSSON, T., AND J. H. GINNS. 1979. Cellulolytic activity and the taxonomic position of selected brown-rot fungi. *Mycologia* 71:170–177.
- NOBLES, M. K. 1965. Identification of cultures of wood-inhabiting Hymenomycetes. *Can. J. Bot.* 43:1097–1139.
- NOBLES, M. K. 1971. Cultural characters as a guide to the taxonomy of the Polyporaceae. Pages 169–196 in *Evolution in the higher basidiomycetes* (R. H. Petersen, ed.). Univ. of Tennessee Press, Knoxville.
- NUÑEZ, M., AND L. RYVARDEN. 1995. *Polyporus* (Basidiomycotina) and related genera. *Synopsis Fungorum* 10:1–85.
- OLMSTEAD, R. G., B. BREMER, K. M. SCOTT, AND J. D. PALMER. 1993. A molecular systematic analysis of the Asteridae sensu lato based on *rbcL* sequences. *Ann. Mo. Bot. Gard.* 80:700–722.
- OVERHOLTS, L. O. 1953. The Polyporaceae of the United States, Alaska, and Canada. Univ. of Michigan Press, Ann Arbor.
- PAGEL, M. 1994. Detecting correlated evolution on phylogenies: A general method for the comparative analysis of discrete characters. *Proc. R. Soc. London* 255:37–45.
- PAGEL, M. 1997. Inferring evolutionary processes from phylogenies. *Zool. Scr.* 26:331–348.
- PEGLER, D. N. 1983. The genus *Lentinus*, a world monograph. *Kew Bull. Add. Ser.* 10:1–281.
- PETERSEN, R. H. 1995. There's more to a mushroom than meets the eye: Mating studies in the Agaricales. *Mycologia* 87:1–17.

- PETERSEN, R. H., AND D. BERMUDEZ. 1992. Intercontinental compatibility in *Panellus stypticus* with a note on bioluminescence. *Persoonia* 14:457–463.
- RAJCHENBERG, M. 1994. A taxonomic study of the subantarctic *Piptoporus* Polyporaceae, Basidiomycetes) II. *Nord. J. Bot.* 15:105–119.
- RAPER, C. A., J. R. RAPER, AND R. E. MILLER. 1972. Genetic analysis of the life cycle of *Agaricus bisporus*. *Mycologia* 64:1088–1117.
- RAPER, J. R., AND A. S. FLEXER. 1971. Mating systems and evolution of the basidiomycetes. Pages 149–168 in *Evolution in the higher basidiomycetes* (R. H. Petersen, ed.). Univ. of Tennessee Press, Knoxville.
- RAYNER, A. D. M., AND L. BODDY. 1988. Fungal decomposition of wood: Its biology and ecology. John Wiley and Sons, Chichester, U.K.
- REDHEAD, S. A., AND J. H. GINNS. 1985. A reappraisal of agaric genera associated with brown rots of wood. *Trans. Mycol. Soc. Jpn.* 26:349–381.
- REE, R., AND M. J. DONOGHUE. 1998. Step matrices and the interpretation of homoplasy. *Syst. Biol.* 47:582–588.
- REE, R., AND M. J. DONOGHUE. 1999. Inferring rates of change in flower symmetry in asterid angiosperms. *Syst. Biol.* 48:633–641.
- RENVALL, P., T. RENVALL, AND T. NIEMELÄ. 1991. Basidiomycetes at the timberline in Lapland 2. An annotated checklist of the polypores of northeastern Finland. *Karstenia* 31:13–28.
- RYVARDEN, L. 1980. A preliminary polypore flora of East Africa. *Fungiflora*, Oslo.
- RYVARDEN, L. 1991. Genera of polypores: Nomenclature and taxonomy. *Synopsis Fungorum* 5: 1–363.
- RYVARDEN, L., AND R. L. GILBERTSON. 1994. European polypores, part 2. *Fungiflora*, Oslo.
- SANDERSON, M. J. 1995. Objections to bootstrapping phylogenies: A critique. *Syst. Biol.* 44:299–320.
- SILLÉN-TULLBERG, B. 1993. The effect of biased inclusion of taxa on the correlation between discrete characters in phylogenetic trees. *Evolution* 47:1182–1191.
- SIMPSON, J. A. 1996. Wood decay fungi. Pages 95–136 in *Fungi of Australia*, volume 1B. (A. E. Orchard, K. Mallett, and C. Grgurinovic, eds.). Australian Biological Resources Study, Canberra.
- SINGER, R. 1986. The Agaricales in modern taxonomy. 4th ed. Koeltz Scientific Books, Koenigstein.
- SOLTIS, D. E., P. S. SOLTIS, M. E. MORT, M. W. CHASE, V. SAVOLAINEN, S. B. HOOT, AND C. M. MORTON. 1998. Inferring complex phylogenies using parsimony: An empirical approach using three large DNA data sets for angiosperms. *Syst. Biol.* 47:32–42.
- STALPERS, J. A. 1978. Identification of wood-inhabiting Aphylophorales in pure culture. *Stud. Mycol.* 16:1–248.
- STALPERS, J. A. 1992. *Albatrellus* and the Hericiaceae. *Persoonia* 14:537–541.
- SULLIVAN, J. 1996. Combining data with different distributions of among-site rate variation. *Syst. Biol.* 45:375–380.
- SWANN, E. C., AND J. W. TAYLOR. 1993. Higher taxa of basidiomycetes: An 18S rRNA gene perspective. *Mycologia* 85:923–936.
- SWANN, E. C., AND J. W. TAYLOR. 1995. Phylogenetic perspectives on basidiomycete systematics: Evidence from the 18S rRNA gene. *Can. J. Bot.* 73 (Suppl.):s862–s868.
- SWOFFORD, D. L. 1999. PAUP* 4.0 Phylogenetic analysis using parsimony, version 4.0b. Sinauer Associates, Sunderland, Massachusetts.
- SWOFFORD, D. L., AND W. P. MADDISON. 1992. Parsimony, character-state reconstructions, and evolutionary inferences. Pages 186–223 in *Systematics, historical ecology, and North American freshwater fishes* (R. J. Mayden, ed.). Stanford Univ. Press, Palo Alto, California.
- SZKLARZ, G. D., R. K. ANTIBUS, R. L. SINSABAUGH, AND A. E. LINKINS. 1989. Production of phenol oxidases and peroxidases by wood-rotting fungi. *Mycologia* 81:234–240.
- TANESAKA, E., H. MASUDA, AND K. KINUGAWA. 1993. Wood degrading ability of basidiomycetes that are wood decomposers, litter decomposers, or mycorrhizal symbionts. *Mycologia* 85:347–354.
- TEMPLETON, A. 1983. Phylogenetic inference from restriction endonuclease cleavage site maps with particular reference to the evolution of humans and the apes. *Evolution* 37:221–224.
- THORN, R. G., J.-M. MONCALVO, C. A. REDDY, AND R. VILGALYS. 2000. Phylogenetic analyses and the distribution of nematophagy support a monophyletic Pleurotaceae within the polyphyletic pleurotid–lentoid fungi. *Mycologia* 92:241–252.
- TOKIMOTO, K., AND M. KOMATSU. 1978. Biological nature of *Lentinus edodes*. Pages 445–459 in *The biology and cultivation of edible mushrooms* (S. T. Chang and W. A. Hayes, eds.). Academic Press, New York.
- TROJANOWSKI, J., K. HAIDER, AND A. HÜTTERMAN. 1984. Decomposition of ¹⁴C-labelled lignin, holocellulose and lignocellulose by mycorrhizal fungi. *Arch. Microbiol.* 139:202–206.
- WATLING, R. 1982. Taxonomic status and ecological identity in the basidiomycetes. Pages 1–32 in *Decomposer basidiomycetes: Their biology and ecology* (J. C. Frankland, J. N. Hedger, and M. J. Swift, eds.). Cambridge Univ. Press, Cambridge.
- WELLS, K. 1994. Jelly fungi, then and now! *Mycologia* 86:18–48.
- WERDELIN, L., AND B. S. TULLBERG. 1995. A comparison of two methods to study correlated discrete characters on phylogenetic trees. *Cladistics* 11:265–277.
- WHITE, T. J., T. D. BRUNS, S. B. LEE, AND J. W. TAYLOR. 1990. Amplification and direct sequencing of fungal ribosomal genes for phylogenetics. Pages 315–322 in *PCR protocols* (M. A. Innis, D. H. Gelfand, J. J. Sninsky, and T. J. White, eds.). Academic Press, San Diego.
- WORRALL, J. W., S. E. ANAGNOST, AND R. A. ZABEL. 1997. Comparison of wood decay among diverse lignicolous fungi. *Mycologia* 89:199–219.
- WU, Q., K. W. HUGHES, AND R. H. PETERSEN. 1995. A reevaluation of taxa of *Clavicornia* subg. *Ramosa* based on morphology, compatibility, and laccase electrophoretic patterns. *Sydowia* 47:89–124.

Received 13 July 1999; accepted 10 February 2000
Associate Editor: R. Olmstead

APPENDIX. LITERATURE SOURCES FOR DECAY MODE, MATING TYPE, AND SUBSTRATE RANGE CHARACTERS

Breitenbach and Kranzlin (1995), Brodie (1975), Burdall and Miller (1975), Casselton and Kues (1994), Coker and Couch (1928), Eriksson et al. (1981, 1984), Esser (1967), Esser and Blauch (1994), Gilbertson (1981), Gilbertson and Ryvarden (1986, 1987), Ginns (1997),

Ginns and Lefebvre (1993), Hibbett et al. (1994), Jülich and Stalpers (1980), Kerrigan and Ross (1988), Larsen and Gilbertson (1977), Martin and Gilbertson (1976), Miller (1971), Miller and Stewart (1971), Nakasone (1990), Nobles (1965), Nuñez and Ryvardeen (1995), Petersen and Bermudes (1992), Rajchenberg (1994), Raper et al. (1972), Rayner and Boddy (1988), Redhead and Ginns (1985), Ryvardeen (1980), Ryvardeen and Gilbertson (1994), Simpson (1996), Stalpers (1978, 1992), Tanesaka et al. (1993), Tokimoto and Komatsu (1978), Trojanowski et al. (1984), Wells (1994), Worrall et al. (1997), Wu et al. (1995).